מכון ויצמן למדע
WEIZMANN INSTITUTE OF SCIENCE

Thesis for the degree
Master of Science

עבודת גמר (תזה) לתואר
מוסמך למדעים

By
Efrat Ramati

מאת
אפרת רמתי

תמורות בין קיבוע פחמן והמאזן הקרינתי בהשפעה על האקלים לאורך גרדיאנט המשקעים בישראל

Tradeoffs between Carbon Sequestration and Radiation Budget in Influencing Climate along the Precipitation Gradient in Israel

Advisor:
Prof. Dan Yakir

מנחה:
פרופ' דן יקיר

January 2015

טבת התשע"ה

Submitted to the Scientific Council of the
Weizmann Institute of Science
Rehovot, Israel

מוגשת למועצה המדעית של
מכון ויצמן למדע
רחובות, ישראל

Acknowledgments

I would like to extend my gratitude to the many people who helped to bring this research project to completion.

First, I would like to thank my advisors, Prof. Dan Yakir and Dr. Eyal Rotenberg for their support, guidance and advice throughout my graduate studies at the Weizmann Institute of Science. A special gratitude is owed to Shani Rohatyn, my mobile lab partner. I would also like to thank the Yakir group members, Yakir, Fyodor, Gil, and Efrat for many fruitful discussions, and especially to Yetti which helped a lot with statistical work in this research. Especially I would like to thank the expert team:Avram Pelner and Hagay Sagi, which supported technical requirements.

Finally and most importantly, I would like to thank my family. Without their love, patience and continuous encouragement this work would not have been possible.

List of symbols and abbreviations

ICG	Israeli Climatic Gradient
$\Delta_{(F-S)}$	Difference between forest ecosystem and the shrub land ecosystem
IMS	Israeli Meteorological Services
Met	meteorological
P	precipitation (mm)
T	temperature (ºC)
RH	relative humidity (%)
Eg	global incoming shortwave radiation
GPP	gross primary production (g C m^{-2})
NEE	net ecosystem exchange (g C m^{-2})
NEP	net ecosystem productivity/ carbon gain (NEP=-NEE) (g C m^{-2})
ET	evapotranspiration
Rn	whole surface (canopy/shrub land) net radiation (W m^{-2})
S_n	net shortwave radiation (W m^{-2})
L_n	net long wave radiation (W m^{-2})
S↓	shortwave radiation received from the atmosphere (W m^{-2})
S↑	shortwave radiation reflected by the surface (W m^{-2})
α	surface albedo, S↑ / S↓ [-]
L↓	long wave radiation received from the atmosphere (W m^{-2})
L↑	long wave radiation emitted by the surface (W m^{-2})
SEB	surface energy balance
H	sensible heat flux (W m^{-2})
H_F	sensible heat flux above forest canopy (W m^{-2})
H_S	sensible heat flux above shrub land (W m^{-2})
r_a	Aerodynamic resistance above the canopy
T_{eco}	ecosystem (surface) temperature (K)
T_{air}	air temperature (K)
LE	latent heat flux, measured evapotranspiration expressed in energy units (W m^{-2})
LV	latent heat of vaporization (J g^{-1})
β	Bowen ratio, H/LE [-]
G	soil heat flux determined as the rate of change of soil heat (W m-2)
EC	eddy covariance

u_*	Friction velocity (m s^{-1})
c_p	Heat capacity of air
ρ_a	air density (g m^{-3})
ρ_c	CO_2 density (g m^{-3})

Abstract

Recent observations from the semi-arid region in Israel showed that conversion of the local sparse shrub land to pine forest resulted in greatly increased surface radiation load due to reduced canopy albedo and reduced emission of thermal radiations, which overwhelmed the beneficial effects of the forests high rates of carbon sequestration. Here we extend this study across the local climatic gradient in Israel, and test the hypothesis that the surface radiation effect of forestation diminishes, while the benefits of carbon sequestration of forestation enhances with increasing precipitation.

We used a custom-built mobile laboratory (for eddy-flux and surface radiation measurements) on a campaign basis (about two weeks per site repeated along the seasonal cycle) to examine the surface-atmosphere radiative (short- and long-wave radiation) and non-radiative (net carbon uptake, NEE, latent heat, LE, and sensible heat, H) fluxes. The research conducted in three paired sites of pine forest *(Pinus halepensis)* and nearby non-forested ecosystem with mean annual precipitation of 291, 543, and 755 mm, and temperature of 19.5, 20.8, and 16.4 ˚C, respectively.

Forest NEE and LE increased with increasing precipitation along the gradient from 0.8, to 1.5 gC m^{-2} d^{-1}, and 0.7 to 1.3 mmol H_2O $m^{-2}s^{-1}$. Forest albedo did not change along the gradient (α_F ~0.12) or along the seasonal cycle, while shrub land albedo (α_S) varied along the gradient and the seasonal cycle due to variability in soil types (from 0.31 to 0.19, on average for dry and wet sites). Sensible heat flux between the sites did not markedly change (sites average: H_F~110 Wm^{-2} and H_S~60 Wm^{-2}), and the net thermal radiation emission along the climatic gradient increased in the forests (90, to 105 Wm^{-2}) and decreased in the shrub land (112 to 104 Wm^{-2}).

The results showed that, on average, enhanced carbon sink associated with forestation (ΔNEP_{F-S}) increased with precipitation (from near zero to 190%) and, concurrently, effect on albedo diminished ($\Delta\alpha_{F-S}$, from ~150 to 50%), which both were associated with changes in plant cover and differences in soil surfaces. Forests always showed higher sensible heat flux compared to shrub land (ΔH_{F-S}~50 Wm^{-2}), while the reduced thermal radiation emission associated with forestation attenuated with increasing precipitation along the gradient from -20 to ~0 Wm^{-2}.

The results confirm our hypothesis about the effect of precipitation gradient on carbon gain and radiation load and help to quantify the interactions of forestation and climate. This study also demonstrates the utility of the new mobile lab, and the importance of extending measurements in permanent sites with limited biome and climatic coverage.

Table of Contents

Introduction

Human activities have been contributing significantly to the alterations of the chemical composition of the atmosphere (Ramanathan et al., 2008). Due to anthropogenic greenhouse gas emissions, the global average atmospheric CO_2 concentration has risen from ~310 ppm to ~400 ppm over the last 50 years (Steffen et al., 2007), playing an important role in modifying the loss of thermal energy from the earth and consequently in global warming. However, the increase in atmospheric CO_2 is significantly smaller than the annual anthropogenic CO_2 emissions due to the existence of natural carbon sinks, in the ocean and in the land, which remove about 50% of the anthropogenic greenhouse gas and, in turn, reduces the absorbed thermal radiation by the atmosphere (Canadell et al., 2007). In this context, terrestrial ecosystems function as important carbon sinks as much of the carbon uptake occurs through its accumulation in vegetation biomass and soil organic matter (Le Quéré et al., 2009). Although forests cover only about a third of the land surface (Bonan, 2008), they sequester large amounts of carbon annually and are responsible for ~50% of the terrestrial net carbon gain (Field and Raupach, 2004). Thus, they can help mitigate climate change (Ballantyne et al., 2012; Bonan, 2008; Canadell et al., 2007; Pan et al., 2011).

The overall amount of carbon being transported vertically between the atmosphere and the biosphere is also known at the ecosystem level as the net ecosystem exchange, NEE. The NEE is the sum of two opposing fluxes: CO_2 uptake through gross primary productivity, GPP, and CO_2 release through ecosystem respiration, R_e (Reichstein et al., 2005), with the balance varying significantly between different land covers (Beer et al., 2010). High GPP is often associated with forest carbon sink, but in fact it is the net carbon exchange, NEE, that accounts for the sink. For example, Rotenberg and Yakir (2010) report similar NEE values of -2.3, and -2.0 ton C ha^{-1} for semi-arid, and European pine forests, respectively (the negative sign denotes a flux from the atmosphere to the earth surface) in spite of significantly lower GPP in the semi-arid ecosystem.

The balance between GPP and R_e is dependent on a set of environmental factors, including temperature, atmospheric demand for moisture and soil moisture availability (Bonan, 2008). Thus, these physical parameters may affect the biological carbon uptake by the ecosystems across climatic gradients. A study across a wide climatic gradient in New Mexico showed that NEE increases dramatically with elevation and mean annual precipitation (Anderson- Teixeira et al., 2011). This directly reflects a negative correlation of NEE with temperature (T) in water-limited ecosystems and a positive correlation of NEE with humidity. Hence, it was suggested that in semiarid ecosystem, where water deficiency and temperature tend to be inversely correlated, where hot and dry conditions inhibit

the accumulation of significant carbon stocks, whereas cooler and wetter conditions favor GPP over R_e, resulting in more carbon buildup (Anderson- Teixeira et al., 2011; Conant et al., 1998).

In addition to their function as a major carbon sink, forests may alter climate through changes in surface energy budget, which consists of radiative and non-radiative energy fluxes. Considering radiative energy, land surfaces receive shortwave solar radiation (S) during daytime and exchange longwave radiation (L) continuously with the atmosphere (Monteith and Unsworth, 1990).The net radiation absorbed by the land as a consequence of these exchanges is often denoted R_n, and the partitioning of net radiation into non-radiative fluxes in the surface energy balance (SEB) is commonly written as:

$$R_n = S_n + L_n = G_0 + H + LE \quad (1)$$

where S_n and L_n are the net shortwave and net longwave radiation fluxes, respectively. The right hand side of the equation describe the non-radiative energy fluxes: G_0 is the soil heat flux, H is the sensible heat flux, and LE is the latent heat flux L is the latent heat of vaporization, and E is the rate of evapotranspiration), which is constrained by water availability (Ma et al., 2002). Since the net surface energy budget must be balanced, the radiative fluxes constrain the sum of the sensible (H) and latent heat (LE) fluxes, together with the soil heat flux (G_o). The estimation of the two atmospheric turbulent fluxes, H and LE, at land surface has long been recognized as the critical step in the determination of the energy and mass exchange between the atmosphere and the biosphere (Monteith, 1965; Montgomery, 1948). It is also important to note that each of these fluxes can be estimated independently (Kiehl and Trenberth, 1997).

The net solar radiation (Sn, Eq.2) absorbed by land surface, defined as the difference between incoming and outgoing shortwave radiative fluxes, is positively related to the local incoming solar radiation flux and negatively correlated with the surface reflectivity, known as albedo (α [defined as ratio between the outgoing solar radiation flux and the incoming solar radiation flux $S_{\uparrow}/S_{\downarrow}$], Eq.2):

$$Sn = S\downarrow(1-\alpha) \quad (2)$$

where incident solar radiation flux ($S_{\downarrow}$) is mainly affected by the location on Earth and the atmospheric conditions. (i.e. aerosols and clouds in the atmosphere strongly affect incoming solar radiation before it reaches the surface, reducing $S_{\downarrow}$ (Feng et al., 2013)). However, α is determined by the surface characteristics (e.g. land cover). For example, a study in forests reveals that the α is generally below ~0.2 in such forests (Betts, 2000). However, Otterman (1974) reports albedo of about 0.42 in a bare sandy soil of the Rajasthan desert.

Forests are usually darker than their surrounding non-forested terrain and have lower α (Davin et al., 2007). A six years study (Rotenberg and Yakir, 2011) in the Yatir forest revealed that annual mean soil albedo in the forest area, (α_{soil}), was ~ 0.21 (or 0.24 for similar environments in other places ((Brovkin et al., 2004)). However, the annual mean ecosystem (above forest canopy) albedo, α_{eco}, was 0.11 (~0.1 decrease in mean α above the forest compared with that above the sparse surrounding shrub land in the semi-arid area). This suggests a major difference between forested and non-forested sites in surface albedo, where poor vegetation-covered sites, such as shrub land and desert, are brighter landscapes with a high surface albedo, while albedo remains low for forest sites. Hence, compared to the surrounding terrains, forests are darker and absorb more solar radiation. For this reason, the net absorbed solar radiation, S_n, is higher in forests than in their surrounding terrains. This has a substantial impact on surface net radiation (R_n), and the difference between forest and non-forest in daily R_n can be quite large and vary with the seasonal changes (Claussen et al., 2001). A study in boreal regions (Betts et al., 2007) reports a mean annual R_n of 14 W m^{-2} less in grasslands compared to the adjacent forest, and about 50 W m^{-2} less in agricultural land, compared to the adjacent forest. Modification of vegetation cover changes the absorption of solar radiation (and R_n) as well as its redistribution to the atmosphere through the non-radiative fluxes (mainly as sensible heat, H, and latent heat, LE) to achieve a surface energy balance (Eq.1).

The forest warming arising from the low albedo is offset by strong evaporative cooling in many regions (e.g. tropical forests). Namely, the cooling of the forests is achieved by an increased rate of LE flux (known also as evapotranspiration, ET) from the canopy to the atmosphere (Bonan, 2008; Davin et al., 2007). However, the LE flux is limited by water availability, so that evaporative cooling is restricted in ecosystems with water limitations. Hence, in dry regions where the release of energy as LE is limited, forests are expected to be warmer than their surrounding terrain. Yet, a previous study by Rotenberg and Yakir (2010), in the semi-arid Yatir forest in southern Israel reports that the forest skin temperature was found to be lower than the surrounding shrub land (by ~5˚C on annual average). It was found that the forest warming, in the dry region, is offset by a massive dissipation of energy as sensible heat flux (H), comparing to the background sparse shrub land. Furthermore, the canopy-atmosphere aerodynamic coupling of the forest ecosystem is highly efficient compared to that of the background shrub land, which in turn enhances the massive release of H flux from the forest to the atmosphere. This effect was named by Rotenberg and Yakir (2010) the "convector effect". The efficient aerodynamic coupling in the forest, compared to background shrub land, was reflected in a lower aerodynamic resistance (r_a of about 16 s m^{-1} in Yatir) of the forest surface, caused by the low

density and the open canopy of the forest leading to higher horizontal inhomogeneity of the surface (Rotenberg and Yakir, 2010, 2011).

The negative dependence between the aerodynamic resistance of the surface and the sensible heat flux rate is as follows:

$$H = \rho C_p \frac{(T_{eco} - T_{air})}{r_a} \quad (3)$$

where H is sensible heat, ρ is the density of air ($1.15\ kg\ m^{-3}$), C_p is the heat capacity of air ($1005\ J\ Kg^{-1}{}^{\circ}C^{-1}$), T_{eco} and T_{air} are the ecosystem surface (skin) and the air temperatures ($^{\circ}C$), respectively, and r_a is the aerodynamic resistance ($s\ m^{-1}$, see Jones (1992))

As suggested by the study of Rotenberg and Yakir (2010), the above convector effect may be accompanied with an additional warming (known also as positive forcing) due to thermal effect on the near surface atmosphere. As indicated by equations 4 and 5 below, the lower temperature associated with the cooler canopy of the forest ecosystem, leads to a lower emission of longwave (thermal) radiation ($L_{\uparrow}$), and therefore enhances the net surface energy by increasing L_n (Schimel, 1995):

$$L_n = L_{\downarrow} - L_{\uparrow} \quad (4)$$

$$L_{\uparrow} = \varepsilon_s \sigma (T_s)^4 \quad (5)$$

where $L_{\downarrow}$and $L_{\uparrow}$ are the incoming and outgoing longwave radiations, respectively, ε_s is the surface emissivity, σ is the Stefan-Boltzmann constant (σ =$5.87 \cdot 10^{-8}\ W\ m^{-2}K^{-4}$), T_s is the surface temperature ($^{\circ}K$). The emissivity is equal to one for a perfectly black body, which holds approximately for the soil surface. Note that the $L_{\uparrow}$ depends on surface temperature through the Stefan-Boltzmann relation (Eq. 5), and that L_n is principally negative due to large $L_{\uparrow}$ (Jones, 1992).

As mentioned before (Eq.1) the total heat gain by the surface (R_n) in the forest as compared to the surrounding shrub land, is due to differences in radiative fluxes of both shortwave (S_n) and longwave (L_n) (Kiehl and Trenberth, 1997; Monteith and Unsworth, 1990). Together, the enhanced S_n effect (due to lower albedo) and the suppressed L_n effect (due to cooler surface) described above mentioned increase of the overall annual net radiation absorption by the forest in Yatir site by about ~49W m^{-2} (radiative forcing) compared to the background shrub land (Rotenberg and Yakir, 2010, 2011).

The ambivalent effects of forests on climate change, namely, reduce atmospheric CO_2 concentrations through CO_2 uptake and surface warming through enhanced solar radiation absorption, raises questions regarding the forests' influence on the local and global climates. As noted in the studies above, the forestation in semi-arid regions can have large effects on surface energy balance. Several studies used climatic gradients, such as in precipitation and temperature, as case studies for understanding the fundamental mechanisms through which climate evoke ecosystems and land cover changes. Few

studies also examined how atmosphere-biosphere interactions depend on changes in elevation, and in vegetation cover, along climatic gradients (Austin, 2002; Conant et al., 1998; Holzapfel et al., 2006; Whittaker and Niering, 1975). Considering the albedo and the thermal effects noted above, and their potential forcing on local climate, it is critical to understand how such effects could vary in different environmental conditions, especially in regions with a sharp climatic or environmental gradient, such as the Eastern Mediterranean region (Asaf et al., 2013). Therefore, the function and role of forests in dry areas should be examined in a broader context, using a comparison between forests and other land covers under the same climatic conditions.

Using a Mobile lab (Asaf et al., 2013), a comprehensive study was carried out along the steep Israeli Climatic Gradient (ICG), from the hot and dry conditions in the Northern Negev to the more cool and mesic conditions in the upper Galilee (Annual precipitation along the gradient ranged from 290 mm in the south to 755 mm in the north). This gradient provided a reasonable setting to investigate the response of both forest and non-forest ecosystems to different climate (with focus on differences in temperature and precipitation). The differences in albedo between the forested and non-forested ecosystems are expected to vary between the different sites along the gradient. In the south, the bright natural soil versus dark forests is associated with large albedo changes. In contrast, in the north the albedo change from shrub land to forest is expected to be much smaller. Similarly, the forest net productivity may increase with precipitation from the south to the north in Israel. The reduced difference in albedo and increased difference in net productivity in the more humid regions are expected to change the balance between the albedo and carbon sequestration.

1.1 **Research Objectives**

The main objectives of this study were to investigate how the differences in surface albedo and carbon uptake between forested and non-forested ecosystems may change along the ICG. For this purpose, a state of the art mobile laboratory was employed, containing all the scientific equipment required for the field measurements.

Within this framework the specific objectives of this study were:

1. To provide information on carbon uptake differences between the forested and non-forested ecosystems across the ICG sites.
2. To derive shortwave radiation load associated with forestation of shrub land across the ICG sites, using radiation measurements.
3. To compare quantitatively the albedo/thermal radiation forcing (RF) associated with forestation in the different pine forests across the ICG sites.

2 Methods and Methodology

2.1 Study sites description

The research was conducted in three pine forests across the steep climatic gradient in Israel (Figure.1a); from Birya (Upper Galilee) in the north, through Eshtaol (Shfela) to Yatir (Negev) in the South. *Pinus halepensis* (Aleppo pine) is a common species in the Mediterranean region, considered a drought resistant species (Ne'eman and Trabaud, 2000). Planted *Pinus halepensis* forests (JNF-KKL) in three ecosystems along the ICG were found suitable for this study: (1) the wet Birya in the *Meso-Mediterranean* region, (2) the medium Eshtaol in the *Thermo-Mediterranean* region, and (3) the dry Yatir in the *semi-arid* region. In each site, the pine forest was associated with a nearby non-forested site, which was typically a grassland or sparse shrub land. However, the shrub land soils varied much along the geographical gradient: dark and basaltic soil in wet Birya, grey-stony cover in the humid Eshtaol, and bright soil in the semi-arid desert of Yatir.

The three forests are of similar age and are planted in the same species *(Pinus halepensis)* but differ mainly in precipitation, from the wettest conditions in Birya to the driest in Yatir (Table 1). During the years 2012, 2013, and 2014 field campaigns were conducted in six separated ecosystems: above forests canopies (Birya, Eshtaol, and Yatir), and at their non-forested surrounding area (Kadita, Modi'in, Yatir desert), respectively. Each campaign was held for about ten days and at least for one week. All measurements were repeated several times a year (mainly in the spring and in the summer) to assess seasonal effects (Table 2). The comprehensive study included measurements of meteorological data, solar and thermal radiation, energy and mass fluxes (carbon dioxide, water, sensible and latent heat).

Table 1.Study sites description. Basic information regarding the three study sites across the Israeli climatic Gradient (ICG). Each site contains two ecosystems: Forest, and shrub land.
* Mean annual rainfall was averaged over the last fifty years.

Site	**Yatir**	**Eshtaol**	**Birya**
Climatic classification	Semi -arid	Thermo Mediterranean	Meso Mediterranean
Latitude coordinate	31° 20' 49.20" N	31° 47' 34.50" N	33° 00' 00.50" N
Longitude coordinate	35° 03' 07.20" E	35° 00' 11.50" E	35° 30' 40.50" E
Mean annual rainfall (mm)*	291	543	755
Elevation (m)	650	380	755
Forest ecosystem *(dominant species)*	Pine forest (*Pinus halepensis*)	Pine forest (*Pinus halepensis*)	Pine forest *(Pinus halepensis)*
Trees age (y)	45	41	36
Forest density (trees ha^{-1})	350	233	600
Canopy height (m)	10	11	11
Shrub land ecosystem	Grass under heavy grazing	Mixed shrubs (annual vegetation)	Grass under heavy grazing

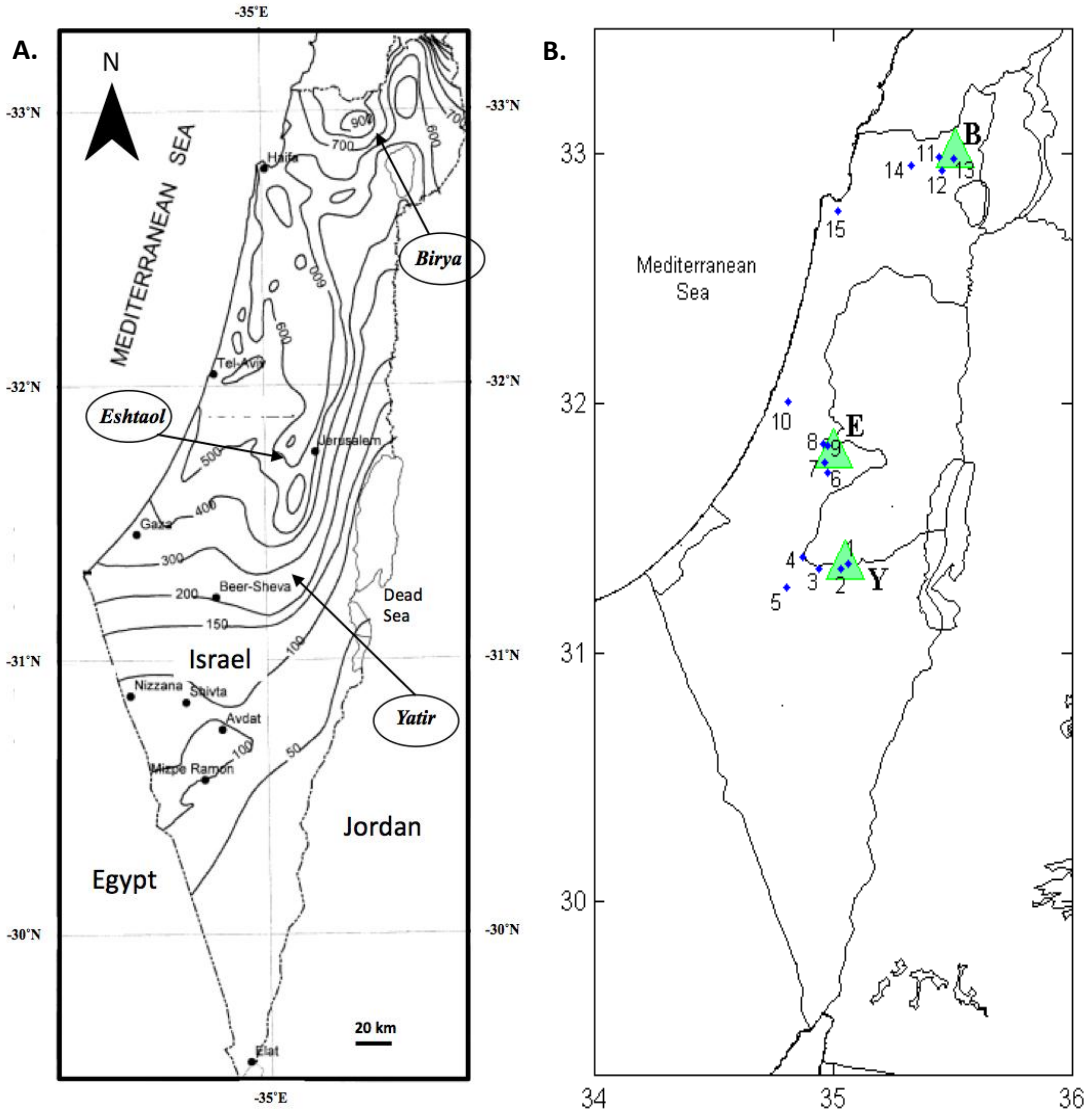

Fig.1. Three study sites and the adjacent meteorological stations along the Israeli Climatic Gradient (ICG). (A) Contour map of mean precipitation (left) with the three study sites (circles): Birya (north), Eshtaol (Shfela), and Yatir (south). (**B)** Fifteen meteorological (IMS-Israeli Meteorological Services) stations (blue dots) distributed around the study sites (green triangles): Yatir (1), Shani (2), Metar (3), Lahav (4), and Beer Sheva Uni. (5) around Yatir site; Beit Jamal (6),Zora (7), Nahshon (8), Latrun (9),and Beit Dagan (10) around Eshtaol site; Meron (11), Amirim (12), Sefat (13), Harashim (14), and Haifa (Technion) around Birya (B).

2.2 **Mobile laboratory**

Field campaigns were relied on the state of the art mobile lab (Fig.2), housed on a 12-ton four-wheel drive truck frame (Girsh Industries, Ashdod, Israel), designed to accommodate laboratory equipment and working conditions. It hosts a pneumatic telescopic mast (4-28m) with complete Eddy covariance (EC) system (gas analyzer, anemometer, and radiation sensors) that can be detached from the lab, racks for instrumentations, computer desk, wireless and cellular communication. The lab is electrically independent using a generator and an uninterrupted power supply (UPS) system.

2.2.1 Flux measurements

The system, which installed at the top of the mast, contains sonic anemometer, gas analyzers, meteorological instruments and air inlets for analytical instruments. A specialized horizontal metal rack was used for the placements of these instruments. Flux measurement relied on an EC system and provides gas and energy fluxes. CO_2, H_2O, sensible and latent heat fluxes are measured using a 3D sonic anemometer (R3-100; Gill Instruments, UK) and an enclosed-path CO_2/H_2O infrared gas analyzer (IRGA; LI-7200, LI-COR Inc., Lincoln, NE, USA) using 60 cm long tubing fitted with 2 μm filter at the inlet (F series, Swagelok, US). The sonic, IRGA and Gill interfaces are linked via either network cable or wireless connection to a computer in the laboratory for data storage and communication to the home lab.

2.2.2 Radiation measurements

The radiation measurements are based on two identical sets of radiation sensors (Kip &Zonen, The Netherland). These are fixed to the specialized rack (installed at the top of the mast) when one facing up while the other facing down. Each of the sets includes solar radiation (0.285-2.80 μm; CMP21), long-wave radiation (4.5-42 μm; CGR4); and photosynthetic a radiation (PAR, 0.4-0.7 μm; PQS1). All sensors are connected using differential mode via a multiplexer to a data logger (CR3000, Campbell Scientific Inc.) and together with the IRGA's air pump are located in a weather-box at the bottom of the mast. Data was recorded and processed, with averages stored every 30 minutes on the CR3000 data logger (Campbell Sci., Logan, UT, USA). Meteorological variables including radiation components were sampled at 1Hz. In addition to the EC system and the radiation sensors, meteorological parameters, such as air pressure, temperature and relative humidity (HMP45C probes, Campbell Scientific Inc., UT, USA) were measured and logged.

2.3 **Eddy covariance flux methodology**

The Eddy covariance method is widely used for measuring exchanges of heat, mass, and momentum between a flat, horizontally homogeneous surface and the overlying atmosphere (Montgomery, 1948; Obukhov and Yaglom, 1959; Swinbank, 1951). Under these conditions, net transport between the surface and atmosphere is one-dimensional and the vertical flux density can be calculated by the covariance between turbulent fluctuations of the vertical wind and the quantity of interest (Foken et al., 2012).

The latent heat, sensible heat flux and CO_2 flux were calculated by the covariance between fluctuations of vertical air velocity *w*, and, respectively, water vapor density *q*, air temperature *T* (extracted from the sonic temperature) and CO_2 concentration, *c* using the formulas:

$$LE = L_V\overline{w'q'} \quad (6)$$

$$H = \rho_a c_p \overline{w'T'} \quad (7)$$

$$F_{CO_2} = \rho_c\overline{w'c'} \quad (8)$$

Where, L_V is the latent heat of water vaporization (2.45 [MJ kg^{-1}]), $\rho_a$is air density, c_p is the heat capacity of air at constant pressure (1.013 10^{-3} [MJ kg^{-1} $^{\circ}C^{-1}$]), and ρ_c is CO_2 density.

The EC technique provides local scale insight to biosphere-atmosphere interactions, is widely used in recent years and allows direct measurements of whole canopy CO_2 and other scalar fluxes (H_2O, sensible heat, and latent heat) in the forest, grassland, desert, and open fields (Beer et al., 2010). The method is based on the assumption that in the mixed boundary layer vertical fluxes of scalars such as water vapor, heat, or CO_2 are approximately constant with height. Thus, the flux measured by a sensor at some point well above the canopy is equal to the flux released or absorbed at the surface. Adequate application of the EC technique requires the validity of the following additional assumptions: the mean vertical air velocity is zero, the terrain is horizontal, the land cover is homogeneous, and sufficient fetch is available upstream of the measurement point.

Using high frequency response sensors, measurements of turbulent fluctuations of vertical velocity and scalar concentration can be performed and their covariance, which represents the vertical turbulent flux, can be calculated. The evapotranspiration (*LE, Eq.6),* sensible heat flux (*H, Eq.7)* and CO_2 flux *(F_{CO2}, Eq.8)* are calculated by the covariance between fluctuations of vertical air velocity and respectively, water vapor density, temperature *T* (extracted from the sonic temperature) and CO_2 concentration.

During nights turbulent conditions are poorly developed. Low turbulence is often characterized by small values of friction velocity (u^*, (Stull, 1988a, b)) which represents the vertical turbulent flux of horizontal momentum. As shown by (Liu and Foken, 2001), at small u^* values considerable uncertainty may be attributed to flux measurements. These authors found that measurements with $u^* < 0.07$ m s^{-1} should be excluded. Hence, at the framework of this study, for each set of measurements a critical friction velocity ($u^*_{(c)}$) was defined (ranged between 0.1-0.2 m s^{-1}), under which flux measurements are highly dependent on the u^* measurements, which corresponded to $u^* < u^*_{(c)}$. These values were considered to be unreliable and were eliminated, while fluxes with $u^* > u^*_{(c)}$ were averaged into a representative constant value which was assigned to the whole night.

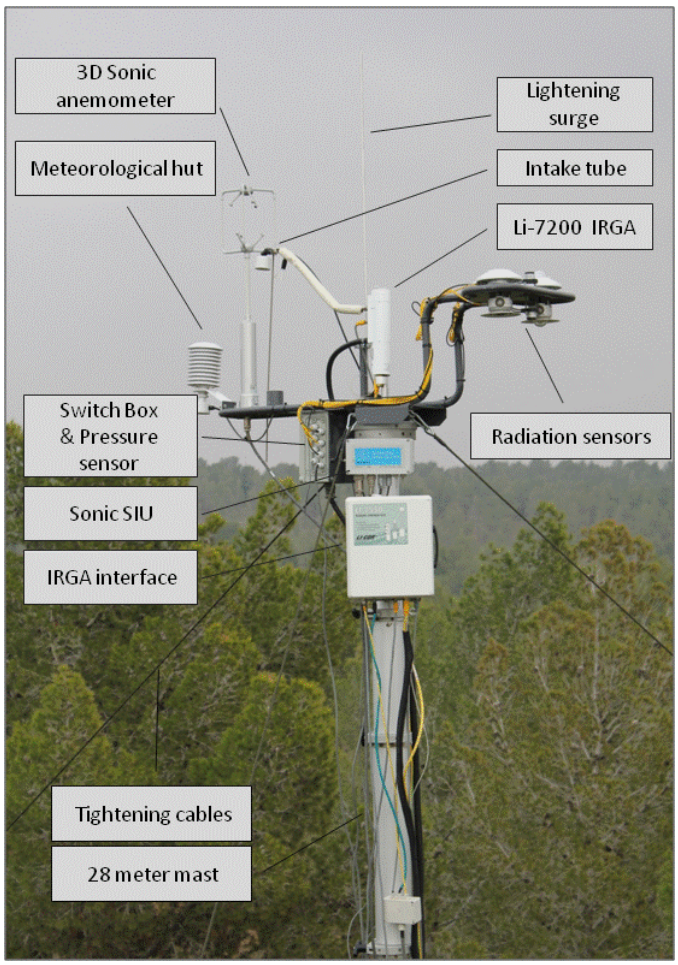

Fig. 2. Measurement mobile system. Measuring components (left) installed on top of the mast: Sonic 3D anemometer, Li-7200 IRGA, six radiation sensors (PAR, long and short wave, up and down) and meteorological hut (air temperature and humidity). The mast opened next to the mobile lab (right bottom).

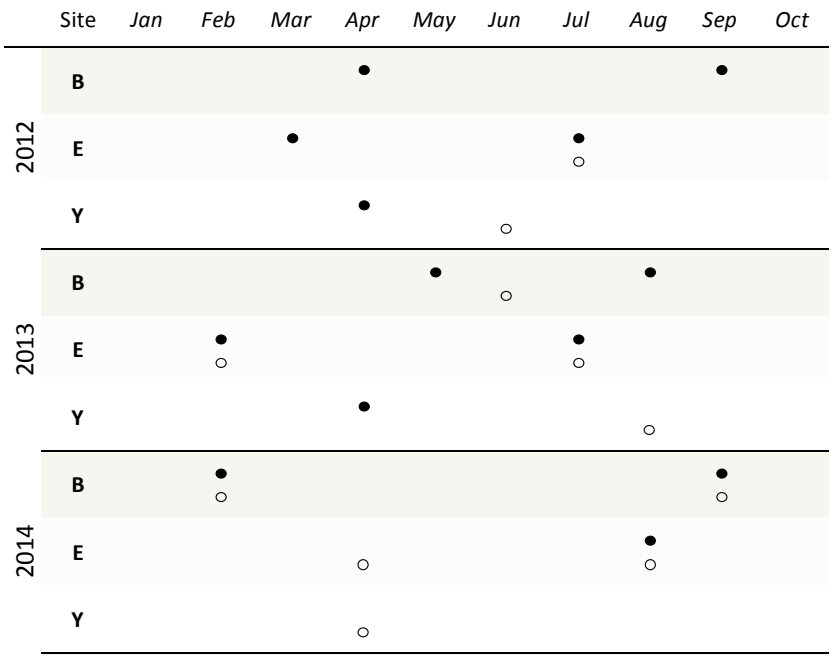

Table 2. Campaigns schedule across the ICG (Israeli Climatic Gradient). Mobile campaigns were conducted during 2012-2014, in three study sites: Birya (B), Eshtaol (E), and Yatir (Y). Each site includes different campaigns in the forest (solid cycles), and shrub land (empty cycles). Campaigns were conducted in the months of Feb-Sep.

2.4 **Data processing**

2.4.1 Energy closure constrain

Verification of the flux measurements can be conducted by the energy balance closure analysis (Wilson et al., 2002). Considering a control volume of the measurement system, the 1st law of thermodynamics (law of energy conservation) at steady state (i.e., neglecting energy storage) shows that the net radiation (R_n) should be balanced by the soil heat flux (G), sensible heat flux (H) and latent heat flux (LE) following the equation:

$$LE + H = (R_n - G) \quad (9)$$

The common method for examining the validity of the EC measurements is the energy balance. In addition to the fluxes measured by the EC technique, net radiation and soil heat flux are measured independently. If the energy balance of the system (Eq.9) is perfectly closed, the flux measurements of H and LE are validated. Hence, the energy closure conflict has become a widely investigated issue. Study by (Wilson et al., 2002) show an average energy balance (EB) deficit of 21% over 22 flux-net sites. The systematic closure problem in the surface energy budget has been reported to reach values of up to 40% of R_n (net radiation) over wheat and grassland (Schwiebus and Berger, 2005; Twine et al., 2000). Among other factors, the possible contribution of non-turbulent heat and vapour transport (mean vertical wind ≠ 0) and spectral losses due to insufficient fetch are possible sources of error. In this frame of work the energy closure was a tool in the quality control process, the calculation was implemented (data points of 30 min averages) without the heat soil flux component (LE + H = Rn), which is rather negligible (G approximately zero in a 24h period).

2.4.2 Data quality control

In addition to EC spike removal procedure, performed by the Eddy Pro software ("Despiking and Raw Data Statistical Screening"), exceptional spikes (H, LE, and CO_2) were removed manually and the missing flux value (30 min average) was adjusted by a linear interpolation. Manual despiking was carried out only for individual cases examined carefully (e.g. when a value does not match, unusually, with the others energy fluxes during the same time). We have made the process of filling gaps that appeared throughout the data series. Gaps in dataset are usually caused due to technical issues (e.g. system stopped functioning, electricity failure etc.) or when excluding night values for low u^*. Small gaps up to 3 hours are filled by linear interpolation. Longer gaps in mobile lab campaigns were not filled.

2.5 **Meteorological data by the Israeli Meteorological Services (IMS)**

Meteorological stations (maintained by the IMS, Fig.1) adjacent to the desired sites (north, shfela, and south) were used to obtain information about basic meteorological parameters such as precipitation (P), temperature (T), relative humidity (RH), and global radiation (Eg). Ongoing data was obtained regarding the period of study (2012-2014) represented as daily mean values (except for P, represented as accumulated daily rain). When more than a single adjacent station dataset were available, the average of the all adjacent stations was calculated. Global radiation (Eg) data were collected from a single adjacent station, where the most suitable station was selected in each site (altitude etc.).

In addition, data sets regarding the mentioned meteorological parameters were processed using a longer period than the years of study (1964-2013). The daily average values for each day of year (365 daily values) were calculated using statistical analysis software (SAS) for all variables except the precipitation (T, RH, and Eg) from the data for the previous 50 years. At the same way both monthly means and yearly means were calculated for the mentioned period. Within this concept, precipitation data were processed in a similar way, this time for the previous 50 years and using accumulated monthly rain. The same approach was applied also for the period of the last 5 years (2009-2013).

3 Results

The following sections report the results, divided into two main topics: (**1**) the climatic gradient as reflected in the three study sites in the basic meteorological variables (precipitation (P), temperature (T), relative humidity (RH), and global incoming solar energy (Eg)) supplied by the Israeli meteorological services (IMS), and (**2**) campaign measurements during the study period 2012-2014, in the three study sites along the climatic gradient.

3.1 **Geographic gradient and time trends across measurement sites**

This study focuses on the effects of the climatic gradient on ecosystem activities. Here we examine the climatic gradient in three major parameters: P, RH and T. We obtained data from the Israeli Meteorological Services (IMS, Beit-Dagan, Israel) measured at 3-6 meteorological (Met) stations which were the nearest to each study sites (Fig.1). The entire available record was examined (Fig. 3). The data show significant inter-annual variations in these three meteorological parameters (P, T, and RH) throughout the last ~50-60 years, with the expected climatic gradient manifested mainly in the P levels: Mean P was 755, 543, and 291 mm; in the moist Mediterranean in Birya, in the dry Mediterranean Eshtaol and, in the semi-arid Yatir, respectively. T was 16.4, 20.8, and 19.5˚C and RH was 58, 62, 61%, following the same sites order. In contrast to local P, in the near surface T and RH records are complicated by factors such as the site elevations (altitudes of ~650, 380, and 755 m for the Birya, Eshtaol, and Yatir sites, respectively). As a result, higher T values are observed in the low altitude Eshtaol site than the higher altitude drier Yatir site. As noted above, considerable inter-annual variations are observed in the met data (Fig.3). The magnitude of inter-annual fluctuations, however, is not the same in the three sites. For example, the Inter-annual variations in P in the different sites seem to correlate with the mean site P. Namely, a higher P level correlates with higher inter-annual variability in P. This is highlighted by the inter-annual anomalies of P (Fig.4). In contrast to the variability in P, as the magnitude of fluctuations in T along the record did not differ significantly between sites, no clear correlation of fluctuation magnitude to site mean T was found. The dependency of the magnitude of RH variations on measurement site was ambiguous, since for all sites RH does not show consistent fluctuations along the inter annual record.

Fig. 3. Inter-annual presentation of: P, T, and RH, across the climatic gradient. Annual averages of entire available record (IMS) are presented above; 60y of P (**active**), and 50y of both T (**b**) and RH(**c**), in the three study sites:Birya (blue), Eshtaol (green), and Yatir (orange). Linear regression shows T trend in the three sites; slopes were 0.0264, 0.0251, and 0.0254 ˚C/y, for Birya, Esthaol, and Yatir, respectively.

Despite the large Inter-annual variations, consistent increasing trend in T was observed in all three sites over last fifty years (~0.03˚C per year for all, on average (Fig. 3), and 0.9, 0.9, and 0.7 ºC, in total over the entire period (Table.3) in Birya, Eshtaol, and Yatir, respectively). In contrast, in spite of the large fluctuations in P, no trend was observed over the entire period. However, RH seem to have trend in part of the record (e.g. since ~1980 decreasing in RH was observed). The existence of observable

time trends in the Met records indicate that this has to be considered in characterizing the background climatic gradient used in assessing the changes in ecosystem activities in our campaign measurements. For this reason we characterized the climatic gradient also for the past five years only (Table 3).

Table 3. Comparison between basic meteorological parameters over different time scales.

	P [mm]		RH [%]		T [˚C]		Eg [W m-2]	
	Inter-annual means (±standard deviations)							
	50y	**5y**	**50y**	**5y**	**50y**	**5y**	**20y**	**5y**
Birya	755 ±29	750 ±80	61 ±0	59 ±2	16.4 ±0.1	17.2 ±0.5	209 ±1	211 ±2
Eshtaol	543 ±21	478 ±41	62 ±1	56 ±1	20.8 ±0.1	21.7 ±0.4	208 ±2	211 ±3
Yatir	291 ±13	255 ±26	58 ±0	58 ±1	19.5 ±0.1	20.2 ±0.4	225 ±1	224 ±3

Table 3 shows the mean inter annual values and their standard deviation. The mean values presented above are both for the entire record of P, RH, T, and Eg (Eg was available only for 20y) and for last 5y period, indicating that the mean values are significantly different. Although there were significant changes between the records, Eg indicates a sustainable average over time.

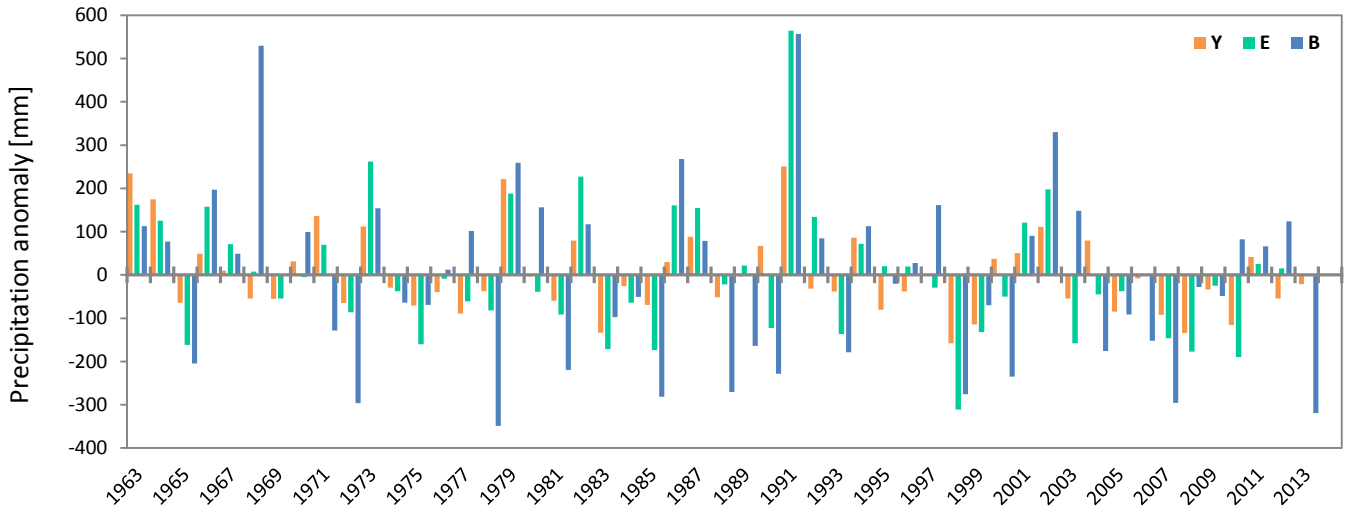

Fig.4.The inter-annual anomaly in precipitation along the ICG sites during 1964-2013. Precipitation data was provided by the Israel Meteorological Services (IMS) using the measurement stations (see supplementary information) around the sites of interest; Birya (**B**), Eshtaol (**E**), and Yatir (**Y**). The 50 y precipitation means from Birya (north) to Yatir (south): 755±29, 543±21, 291 ± 13 mm respectively.

In particular, the mean annual precipitation was lower through the last 5 years than in the last 50 years in all three sites. Fig.4 clearly shows the high negative anomalies of P at about the last decade (since ~2004), in all three sites. Focus on the last 5y reveals the frequent negative values in both Eshtaol, and Yatir, lead to lower P averages in the last 5y. Despite the dramatic negative anomaly in 2013, Birya show mainly positive anomalies in the last 5y, the balance between these trends leads to only small decrease in P comparing to the entire record.

3.1.1 The seasonal cycle in study sites along the climatic gradient

According to the results of this analysis, we characterize the climatic gradient along the seasonal cycle for further use with the campaign results over the last 5 years only:

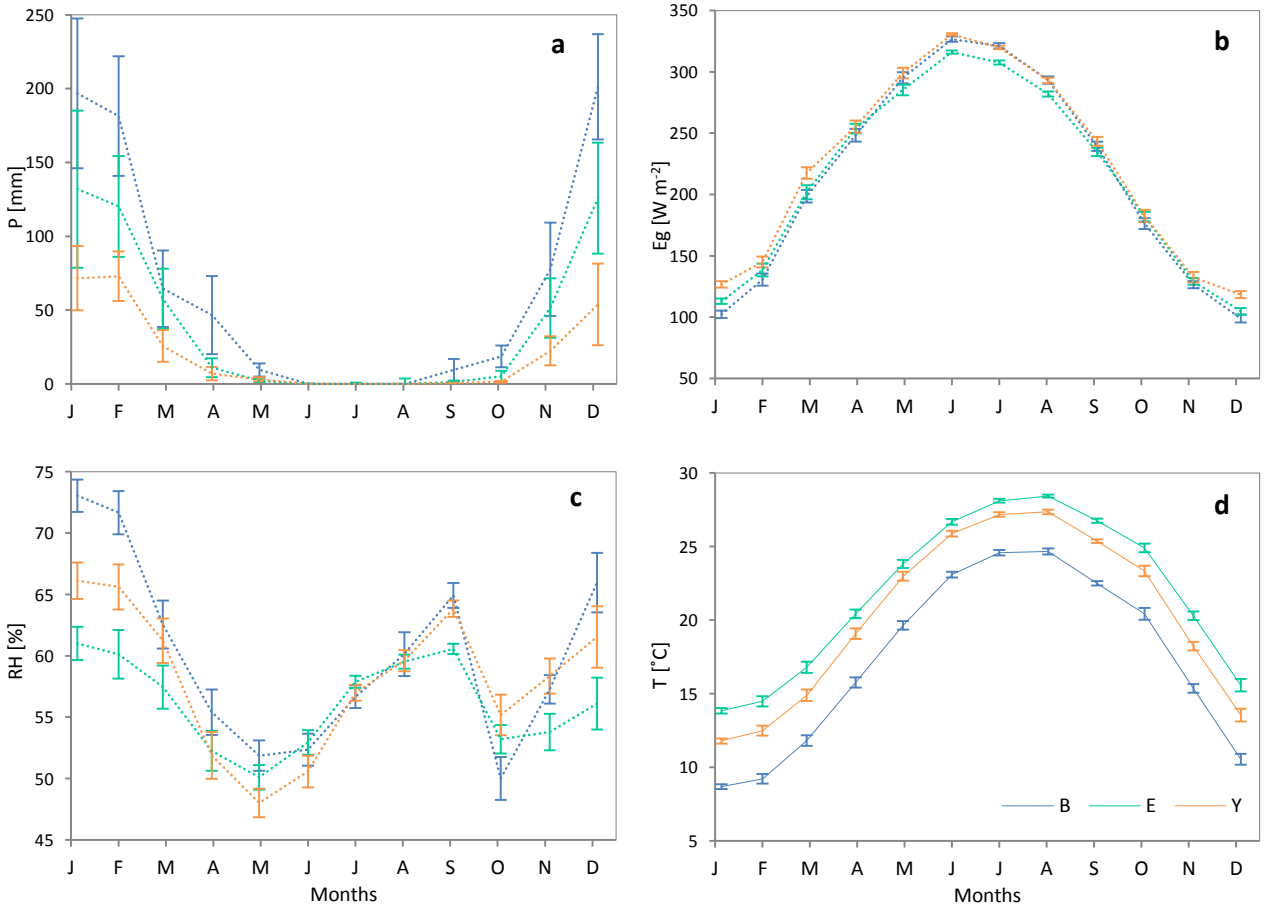

Fig.5.Seasonal cycles of P, RH, Eg, and T in three sites across the gradient. The average seasonal cycles of P, Eg, RH, and T over last five years (2009-2013) along gradient; Birya (blue), Eshtaol (green), and Yatir (orange). Cycles of all three sites were presented by monthly means of daily means of four parameters; (**active**) P, (**b**) Eg, (**c**) RH and (**d**) T. RH in Aug- Dec, 2012 was not available in Birya, so it was calculated from four years only in these months. Error bars indicate standard errors.

Using the record of the last five years as the basis for further evaluation of the climatic gradient, we observe a consistent characteristic seasonal cycles for all three sites. As noted above, the trends in the measured parameters do not clearly reflect the geographic order except for the P because of the elevation effects. Differences between the sites were most significant in P and T seasonal cycle curves and the least in Eg. P (Fig.5a) shows a solid climatic gradient, following the geographical (latitudal) order of the sites during all seasons, when mean P is highest in Birya and lowest in Yatir. Differences between monthly means of P between the sites varied with season; greater differences were observed in winter (Nov-Feb), while during summer (Jun-Aug) all sites are nearly dry so that the gradient cannot be observed.

Fig. 5b indicates an almost similar Eg cycle in all three sites. Still, slight differences in the Eg behavior between the 3 sites were observed: during autumn, winter, and spring (Sep-Apr) Eg was the highest in Yatir and the lowest in Birya. However in late spring and summer (May-Aug) Eg in Eshtaol (lower latitude) was lower than in Birya (higher latitude). Moreover, Eg in Birya was similar to Yatir mostly in summer (May-Sep), but during the rest of the year it was closer to Eshtaol. As can be seen in Fig. 5c, RH is significantly different between the study sites during winter and spring (Dec-May) when conditions are the most humid. In these months Birya has the highest humidity but Eshtaol, rather than Yatir, has the lowest humidity. However, expected climatic gradient in RH was observed only during May. In particular, a strong reduction of RH in October can be observed in all sites, where the most dramatic decrease was in Birya while the shallowest was in Yatir. It is worth noting that the same deep was observed in the other record years (more than 5y ago). This particular month presents an inverse gradient of RH where Yatir was the most humid. Similarly to Eg, the seasonal cycle of T (Fig.5d) shows a consistent difference between the sites. However, this difference did not correlate with the geographic order; the highest T was obtained in Eshtaol and the lowest in Birya. Mean T in Birya was considerably lower than in both Eshtaol and Yatir (e.g. 24.7, 28.4, and 27.4 °C in August for Birya, Eshtaol and Yatir, respectively). Generally, August and January show the max and min T, respectively.

3.2 **Manifestation of the climatic gradient in mobile campaigns data**

The manifestation of the climatic gradient was examined through the measured parameters: NEE, H, LE, Sn, Ln, and Rn in the two main seasons; the active (wet) season, including campaigns during March, April, and May, and the non-active (dry), including campaigns during July, August, and September. The campaigns included 7-32 days of measurements per season per site during 2012-2014. Measurements were performed at the ecosystem scale in three forests (F) and three shrub lands (S) adjacent to these forests, using the Mobile System. In the Yatir forest the forest data were collected by the stationary flux tower system continuously operating at the site over the last fourteen years (Grünzweig et al., 2003).

3.2.1 Carbon exchange

Carbon exchange measurements were conducted conventionally as net ecosystem exchange (NEE, rate of removal of CO_2 from the atmosphere) but for convenience carbon flux was expressed as the ecosystem's carbon gain, i.e., net ecosystem productivity (NEP, where NEP= -NEE) (see Fig. 6).

The forests' mean NEP rate was 2.3 and 0.7 g C m^{-2} d^{-1} in the active, and non-active seasons, respectively. The forests present a steep NEP gradient between the two more humid sites (Birya and Eshtaol) and the dry site in Yatir. On average Eshtaol showed higher NEP values than Birya, but the difference was not significant. The decrease in NEP between the humid and the dry forests in the active season were 29% and 40% from Birya and from Eshtaol to Yatir, respectively. All three forests showed large decrease in NEP in the transition from the active to the non-active season, when the dry forest became a carbon source. The carbon loss in the transition from the active season to the non-active season was the higher in Yatir than in the both Eshtaol and Birya (on average, NEP decreased in about 52, 56, and 112 %, in Birya, Eshatol, and Yatir, respectively). In the non-active season, differences in carbon gain values between the humid forests to the dry Yatir forest were greater than in the active season: 118, and 116 % between Birya, and Eshtaol to the Yatir forest, respectively (where Yatir was a source).

Shrub lands showed a consistent gradient of NEP, which was inverted compared with the forest sites, with the smallest NEP in more humid Birya site to the largest NEP in the dry Yatir site. In the active season, Birya showed essentially neutral system (NEP not significantly different from zero), while the two other sites showed significant carbon gain. In the non-active season, however, shrub lands in all sites were carbon sources. On average, the shrub land sites had a mean NEP rate of 0.7 and -1.2 g C m^{-2} d^{-1} in active and non-active seasons, respectively. Differences in NEP rates in the transition between wet (active) to dry (non-active) seasons in the forests and shrub lands (defines as

ΔNEP_F, and ΔNEP_S, respectively) indicated higher sensitivity to seasonality in Birya and Eshtaol, among shrub lands, while Yatir shrub land showed less sensitivity compare to the forest (ΔNEP_S = -1.9, -2.2, and -1.6 g C m^{-2} d^{-1}, and ΔNEP_F= -1.3, -1.6, and -1.9 g C m^{-2} d^{-1} in Birya, Eshtaol, and Yatir respectively). Overall, the forests mean carbon uptake rate was higher compared with the adjacent shrub lands along the climatic gradient, regardless the season. However, the difference in NEP between forest and shrub land (ΔNEP_{F-S}) changed along the gradient, from ΔNEP_{F-S} of 2.5 g C m^{-2} d^{-1} in Birya, 2.0 g C m^{-2} d^{-1} in Eshtaol and 0.4 g C m^{-2} d^{-1} in Yatir in the active season, and 3.1, 2.6, and 0.1 g C m^{-2} d^{-1} in the non-active season.

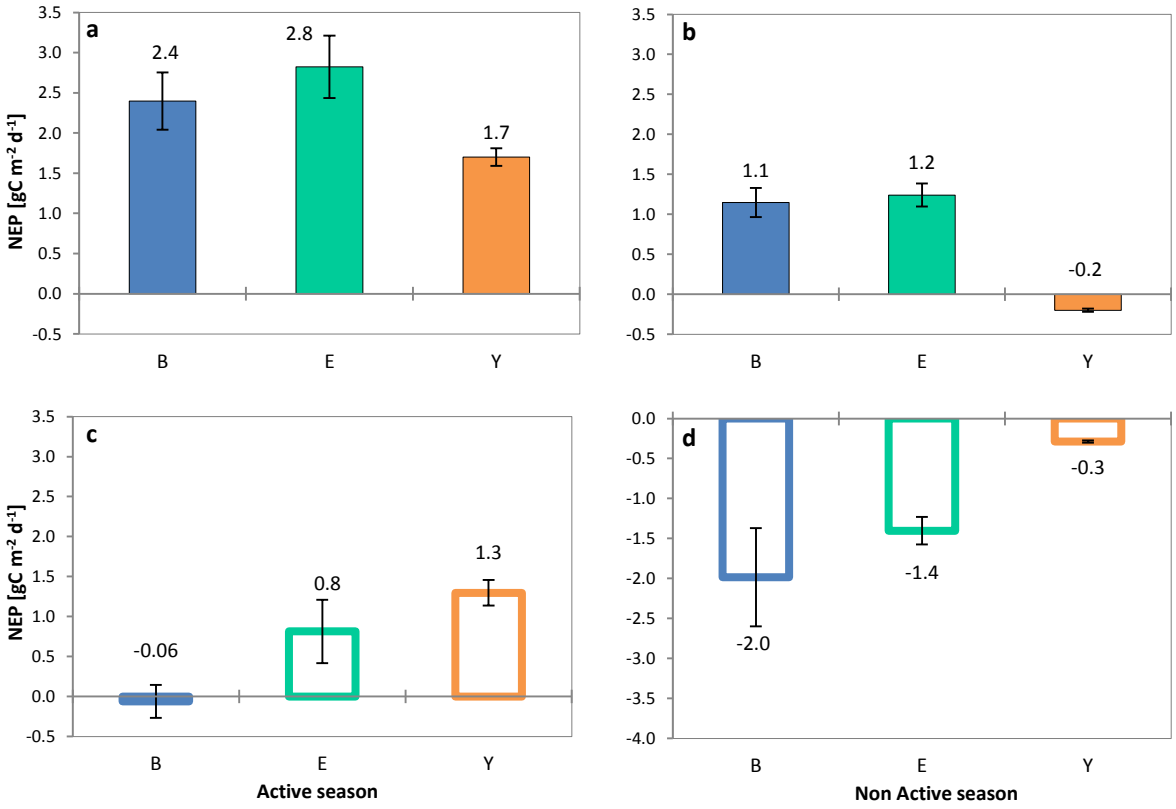

Fig. 6. the net carbon gains across the ICG sites. Seasonal NEP averages of three forests (solid bars) and three shrub lands (empty bars) along the precipitation gradient: Birya (B), Eshtaol (E), and Yatir (Y) during two different seasons. (a) Forests in active season (b) Forest in the non-active season (c) Shrub lands in active season (b) Shrub-lands in the non-active season. Active season included March, April, and May, and the non-active included July, August, and September. All the available NEP data was averaged on the daily (24h) mean scale. Positive NEP indicates carbon sink; Error bars indicate standard errors.

3.2.2 Radiative fluxes

The main four ecosystem-atmosphere radiative fluxes along the gradient, in the three forests and shrub land sites were measured or calculated: Incoming global energy (Eg), net solar radiation (Sn), net long wave radiation (Ln), and the net radiation (Rn).

As seen in Fig.7a and Fig.7b, Eg in the forest sites was on average 259 and 305 W m^{-2} in active and non-active seasons, respectively, representing the expected seasonal changes in incoming solar radiation. Although Yatir shows the highest Eg in the active season, it did not differ significantly from the Eg in Birya, while in Eshtaol Eg was significantly lower. In contrast, in the non-active season differences in Eg between the forest sites were insignificant, when in principle Eg in Eshtaol was the highest. Since the distance between sites is relatively small (~180 km Birya to Yatir) the small within-season differences are likely only due to changes in cloudiness. The forests' mean Sn values were 228 and 280 W m^{-2} in active and non-active seasons, respectively. The Rn values were, on average, 136 and 187 W m^{-2} in the active and non-active seasons, respectively. Similarly to the solar energy components (Eg, and Sn), Rn values in Yatir were the highest, regardless of the season. Assessing Rn as a fraction of total solar radiation load (Rn/Sn) also indicates the highest fraction in Yatir (Rn/Sn was 59, 55 and 60% in the active season and 63, 68, 69% in the non-active season, in Birya, Eshtaol, and Yatir, respectively), with the geographical gradient in ecosystem characteristics more clearly observed in the non-active season. In the same context, in dry site the portion of |Ln| in total solar radiation load (Sn) is smaller than in more humid sites (although Sn is higher). E.g., on average, $|Ln|/Sn$ was 44, 49, and 38% in the active season and, 40, 35, and 29% in the non-active season, in Birya, Eshtaol, and Yatir, respectively. Combined, these radiation fractions clearly indicated the high radiation load in the dry sites, with high absorption load (Rn/Sn) and low thermal emission losses ($|Ln|/Sn$).

Eg values in the shrub lands (Fig.7c and Fig.7d) were on average 269 and 281W m^{-2} in active and non-active seasons, respectively (Eg should be generally the same in forest and shrub land; the differences are related to the dates of campaigns, i.e., they are random). Shrub lands show a gradient in Eg from lower Eg values in the humid Birya site to the higher Eg values in the dry Yatir site, in both seasons, while Eg values in Eshtaol varied with seasonality (lower and higher than the shrub lands' average, in the active and non-active season, respectively). Seasonal differences in Eg between active and non-active season varied among shrub lands, likely due to slight variations in cloudiness during the measurement campaigns: about 8%, 20%, and none, in Birya, Eshtaol and Yatir sites, respectively. The average Sn in the shrub lands was 208 and 211W m^{-2} in active and non-active seasons, respectively.

Rn values in the shrub lands were, on average, 106 and 110 W m^{-2} in active and non-active seasons, respectively. In general, Rn values in Yatir shrub land were consistently higher than in Birya shrub land, whereas the Rn values in Eshtaol shrub land were significantly higher than in both Birya and Yatir shrub lands, regardless of the season.

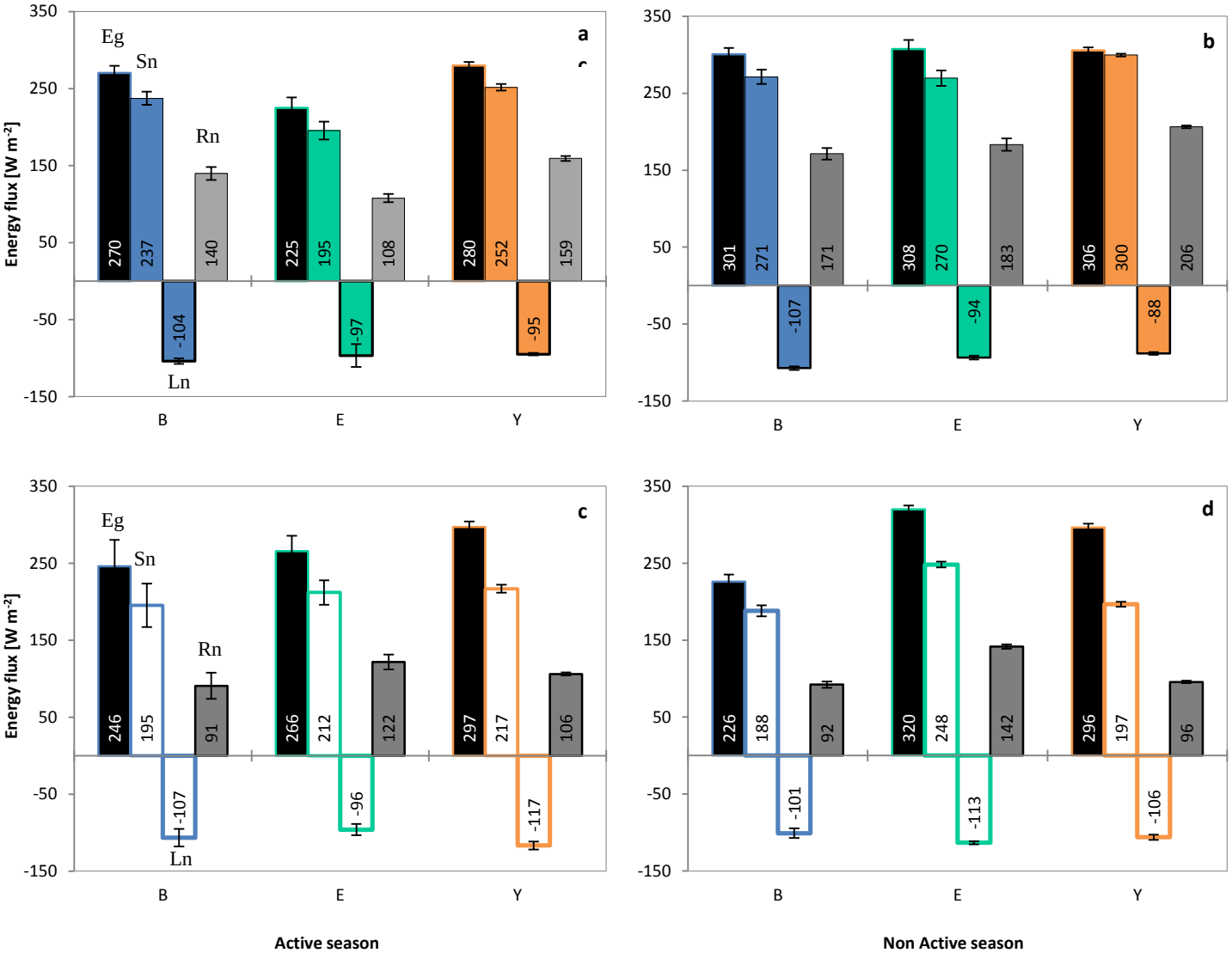

Fig. 7. Radiative energy fluxes in three forests (F) and three shrub lands (S) across the ICG sites.

Seasonally means of incoming global energy (Eg), net solar radiation (Sn), net longwave radiation (Ln), net radiation (Rn). All fluxes were calculated as daily (24h) values. (**a**) Forests in active season (**b**) Forest in the non-active season (**c**) Shrub-lands in active season (**d**) Shrub-lands in the non-active season. Error bars indicate standard errors.

A comparison between the ecosystems (forests and shrub lands, indicated as Δ_{F-S}) along the climatic gradient, in different seasons (i.e. the wet active, and the dry non-active seasons), was used to examine the interactions between the local climatic conditions and land cover characteristics. In general, all the radiation fluxes (Sn, Ln, and Rn) were greater in the forests comparing to the adjacent shrub lands in the non-active season (all sites present positive Δ_{F-S}). In the active season, however, in Eshtaol the shrub land showed greater radiation values than in the forest (Δ_{F-S} was negative). The Δ_{F-S} values for Sn, Ln and Rn were consistently larger in Yatir than in Birya (with exclusion of Sn in active season, apparently due to the different days of measurements), showing clear North-South gradient in ecosystem characteristics. However, the differences in radiation fluxes between forest and adjacent shrub land in the intermediate site of Eshtaol showed negative differences in all energy fluxes, in the active season, and were not always intermediate between the Birya and Yatir sites. The impact of seasonal changes was reflected in the significant increase in Δ_{F-S} values for the different net radiation parameters in the non-active season. Furthermore, the Δ_{F-S} of the net radiation (Rn), in particular, was consistently larger in Yatir than in the other two sites (Δ_{F-S} values of the net radiation (Rn) were 49, -14, and 53 W m^{-2} in the active season,79, 41, and 111 W m^{-2} in the non-active season, in Birya, Eshtaol, and Yatir, respectively).

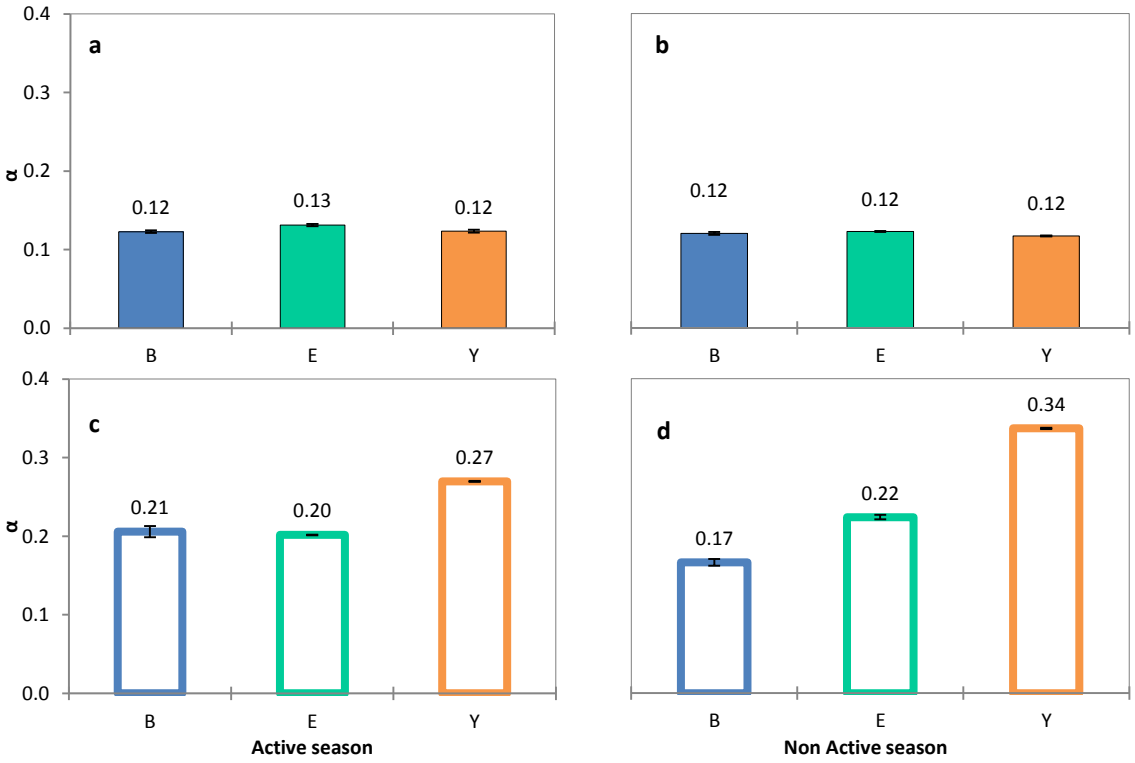

Fig. 8. Albedo across the ICG sites. Seasonal means of albedo (α) in three forests (F, solid bars) and three shrub lands (S, empty bars) along active precipitation gradient. Daily values were calculated by S↑ and S↓ fluxes which conducted over 24h. (**a**) Forests in active season (**b**) Forest in the non-active season (**c**) Shrub-lands in active season (**d**) Shrub-lands in the non-active season. Error bars indicate standard errors.

Differences in albedo (α_f; Fig.8a and 8b) were negligible between the different forest sites, with the albedo in Eshatol slightly higher than in both Birya and Yatir forests. However, albedo values slightly decreased, on average, when going from the active to the non-active season (α_f was, on average, 0.13 in the active and 0.12 in the non-active season). In contrast, albedo in the shrub lands (α_s) (Fig.8c and 8d) was consistently higher than in the forests (α_s were, on average, 0.23 in the active and 0.24 in the non-active season) and with larger variability between the three shrub lands, particularly in the non-active season. The shrub lands present a steep gradient in albedo between the dry Yatir site to the humid Birya and Eshtaol sites. The gradient in α_s was more significant in the non-active season, and it negatively correlated with precipitation**.**

3.2.3 Non radiative fluxes

The dissipation of non-radiative energy was studied through measurement of the two main fluxes: sensible heat flux (H), and the evapotranspiration flux (LE). The forests' average H was 70 and 151W m^{-2} in the active, and non-active seasons (Fig. 9a and 9b), respectively. No clear gradient was observed between the humid forests (Birya and Eshtaol) to the dry forest (Yatir), neither in the active season nor in the non-active season. The differences in H between Eshtaol and the two other forests (Birya and Yatir) were significant: H in Eshtaol was the lowest among forests in the active season (46 W m^{-2} in Eshtaol, compared with 81.5 W m^{-2}, on average in the two other forests), but the highest in the non-active season (191 W m^{-2} in Eshtaol, compared with 130.5 W m^{-2} on average for Birya and Yatir sites). Although the three forests showed significant increase in H values in going from active (wet) to non-active (dry) season, the seasonal variability was much greater in the Eshtaol site (4.2 times increase, compared with 1.5 and 1.8 for Birya and Yatir sites).

Forests mean LE values were 60 and 40 W m^{-2} in the active and non-active seasons (Fig. 9c and 9d), respectively. In contrast to H, the LE fluxes, in both seasons, clearly reflect the North-South precipitation gradient. LE values in Eshtaol and Yatir were 91% and 49% of that in Birya, respectively, in the active season, and 94% and 57%, respectively, in the non-active season. All three forest sites showed large decrease in LE values in the transition from active to the non-active season: by 37%, 36%, and 25%, in Birya, Eshtaol, and Yatir, respectively. In relative terms the dry forest of Yatir showed the lowest seasonal sensitivity in LE.

Shrub land sites along the gradient sites showed mean H fluxes of 50, and 82 Wm^{-2} in the active, and the non-active seasons, respectively. Although shrub land H fluxes in the active season do not show a significant trend along the climatic gradient, in the non-active season the H flux in the Eshtaol site was clearly higher than in both Birya and Yatir (105W m^{-2} in Eshtaol, compared with 69 and 73

W m^{-2} in Birya and Yatir, respectively). Similar to the case of the forest, the Eshtaol shrub land site showed the highest sensitivity on the seasonal scale (increase by 102% from the active to the non-active, compared with increased by only 28%, and 62% in Birya and Yatir sites, respectively).

On average, the LE fluxes in the shrub land sites were: 44 and 16W m^{-2} in active and non-active seasons, respectively. The seasonal decrease in the shrub land LE (from the active to the non-active seasons) indicated the high sensitivity of the dry site: LE in the non-active season was 49% of that in the active season, in both Eshtaol and Birya shrub land sites, but was only 12% in the Yatir site. In contrast to LE in the forests, LE in the shrub land sites did not show a consistent climatic trend: LE in the Birya site was 14% smaller than in the Yatir site in the active season, but 245% larger in the non-active season, and the intermediate Eshatol shrub land showed the largest LE flux in both seasons (21%, and 400% larger than Yatir, in active and non-active, respectively).

The Δ_{F-S} differences in H and LE fluxes generally indicated larger fluxes in the forest sites, but differences were variable across sites and season. For H, the Δ_{F-S} was similar (32 W m^{-2} in the northern and southern sites (Birya and Yatir) but it was -6 W m^{-2} in the intermediate Eshatol site, in the active season. The differences in H were larger in the non-active season: 56 and 63 W m^{-2} for Birya, and Yatir, respectively, and 86W m^{-2} for Eshatol. For LE, the Δ_{F-S} values were 38, 16 and 14W m^{-2} in the Birya, Eshatol and Yatir sites in the active season and 29, 18 and 22W m^{-2} for the same sites in the non-active season.

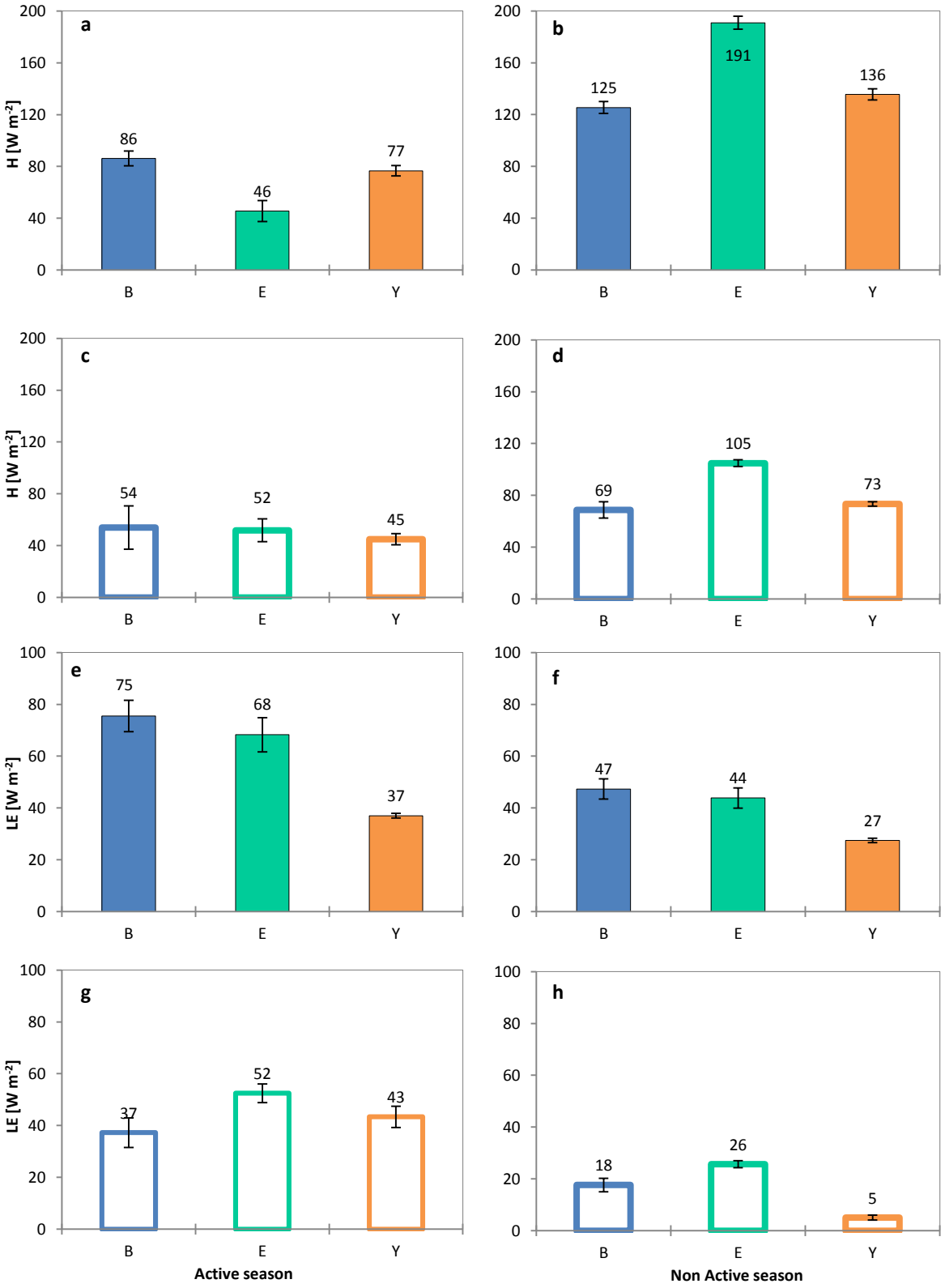

Fig. 9. Non radiative energy fluxes (H, and LE) across the ICG sites. (a) Daily sensible heat, H, and **(e-h)** latent heat, LE, fluxes present as seasonal averages of three forests (F, solid bars) and three shrub lands (S,empty bars) along the precipitation gradient: Birya (B), Eshtaol (E), and Yatir (Y) during two different seasons. (**a,e**) Forests in active season (**b,f**) Forest in the non-active season (**c,g**) Shrub-lands in active season (**d,h**) Shrub lands in the non-active season. Both, H and LE data was averaged on the daily (24h) mean scale. Error bars indicate standard error.

The Bowen ratio (β=H/LE) values of the forests in active season (fig. 10a), and in non-active season are presented in Fig. 10b. The results indicate a significant gradient in β values between the humid forests (Birya and Eshtaol) and the dry forest (Yatir) with higher beta values in the dry forest sites in both the active and non-active seasons, relative to the wetter sites. In all sites - both forest and shrub land - there was a clear increase in β values from the active to the non-active season (by a factor of 2-3). The differences in β values were relatively small between the Birya and Eshtaol forest sites and among all shrub land sites in the active season. β value of the dry Yatir site was significantly larger than in other forests during both seasons and in the shrub land during the non-active season only.

The forest-shrub land differences (Δ_{F-S}) in β values were relatively small during both seasons in the Birya and Eshtaol sites (Fig. 10c). However, the dry Yatir site showed larger Δ_{F-S} values for β: 3.5 and 4.3 for the active and non-active seasons, respectively (compared with Δ_{F-S} values of -1.2 to 1.0 for the other sites).

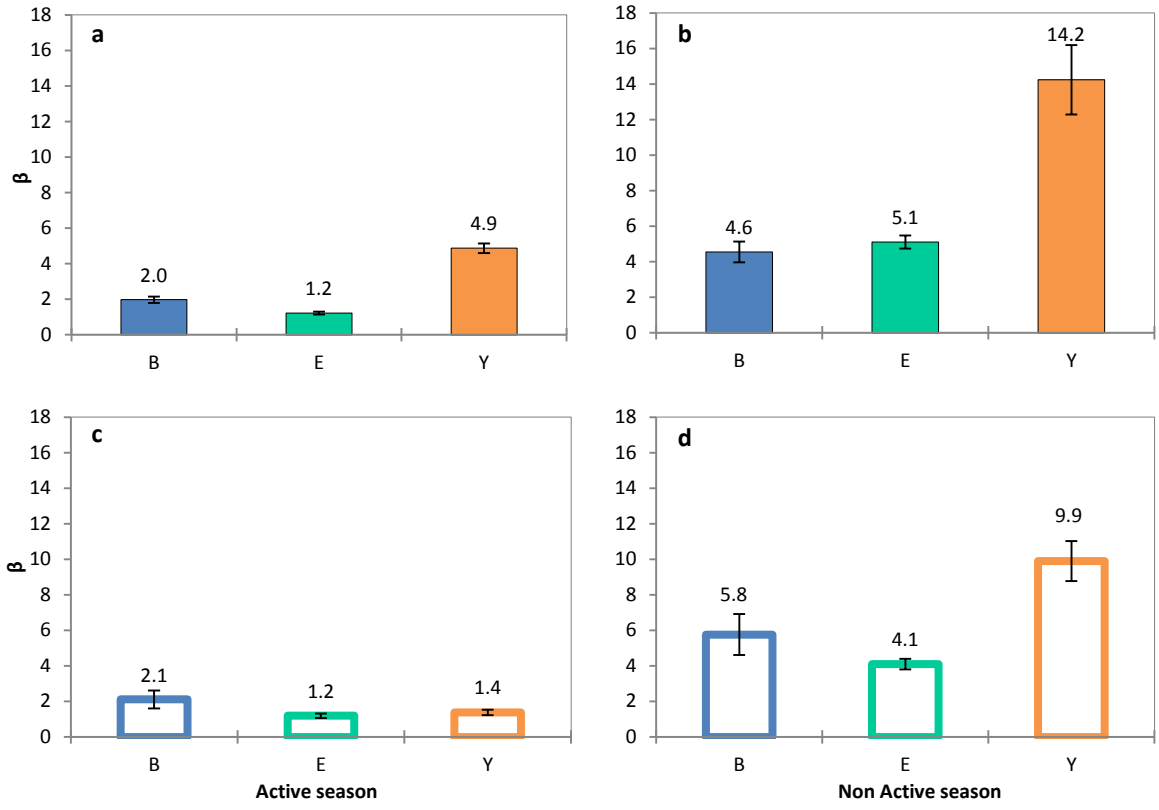

Fig. 10. Bowen ratio across the ICG sites. Seasonal mid-day means Bowen ratio (β= H/LE) in three forests (F) and three shrub lands (S) along active precipitation gradient. Mid-day values were calculated by H and LE fluxes conducted at the peak of day-time (10:00-14:00). (**a**) Forests in active season (**b**) Forest in the non-active season (**c**) Shrub-lands in active season (**d**) Shrub-lands in the non-active season. Error bars indicate standard errors.

4 Discussion

We studied the sensitivity of the effect of land use changes, from shrub land to forest, to environmental conditions along the climatic gradient in Israel. We hypothesized that with increasing precipitation the difference between shrub land and forest will increase in terms of carbon gains, and decrease in terms of surface energy load. For this, we quantified first, the climatic gradient in Israel, and second, the changes in carbon and energy fluxes between shrub land and forests along the gradient.

To quantify the climatic gradient in Israel, we analyzed data from met stations in the vicinity of our measurement sites. In most cases 50 years of data were available. However, many of the met parameters are undergoing change, associated to the global climate change (Myhre et al., 2013). Such trends were indeed observed in temperature and precipitation. In particular, temperature increased by 0.25 ºC/decade over the 50 years record across all sites (Fig.3b). This rate is almost double that of the reported for global mean surface temperature over the same period (Cubasch et al., 2013; Foster and Rahmstorf, 2011; Solomon, 2007). Note that minimum and maximum daily temperatures, or different period during the measurement record may show different rate of change, but this analysis was beyond the scope of this study. In light of these long-term trends, we used the mean values for the last 5 years to represent the climatic gradient during the study period (2012-2014). During this period, the gradient in precipitation was: 750±80, 478±41, and 255±26 mm in Birya, Eshtaol, and Yatir (compared to 755±29, 543±21, and 291±26 for the entire 50 years record; see Table 3). The gradients in temperature and relative humidity (RH) were: 17.2±0.5, 21.7±0.4, and 20.2±0.4 ºC, and 59±2, 56±1, and 58±1%, in Birya, Eshtaol, and Yatir, respectively. As expected there was no gradient in solar radiation due to the small distance between sites (180 km from Birya to Yatir), other than minor changes due to variable cloudiness. Notably, the temperature differences among the sites indicated a possible complication in assessing the trends in ecosystem activities along the gradient. While the intermediate site of Eshtaol fits well along the gradient in P (755±29, 543±21, and 291±26, in Birya, Eshtaol, and Yatir respectively), this was not the case for T (16.4±0.1, 20.8±0.1, and 19.5±0.1ºC, respectively; Fig.3, Table 3). T in Eshtaol is ~1.3 ºC higher than in the semi-arid of Yatir and ~4.5 ºC higher than in Birya. This is likely due to its lower altitude of the site compared to other sites (~650, 380, 755 m, in Birya, Eshtaol, and Yatir, respectively), demonstrating the importance of the elevation parameter in considering climatic factors in general, and in gradient studies in particular (Anderson- Teixeira et al., 2011). Based on the climatic gradient assessed above, we focused on the changes in the impact of the land cover (i.e. shrub land vs forest) on the ecosystem's carbon and energy budget, using the differences between each forest and the local background shrub land (Δ_{F-S}, which was tested for NEP, α, and β) across the climatic gradient (P, and T).

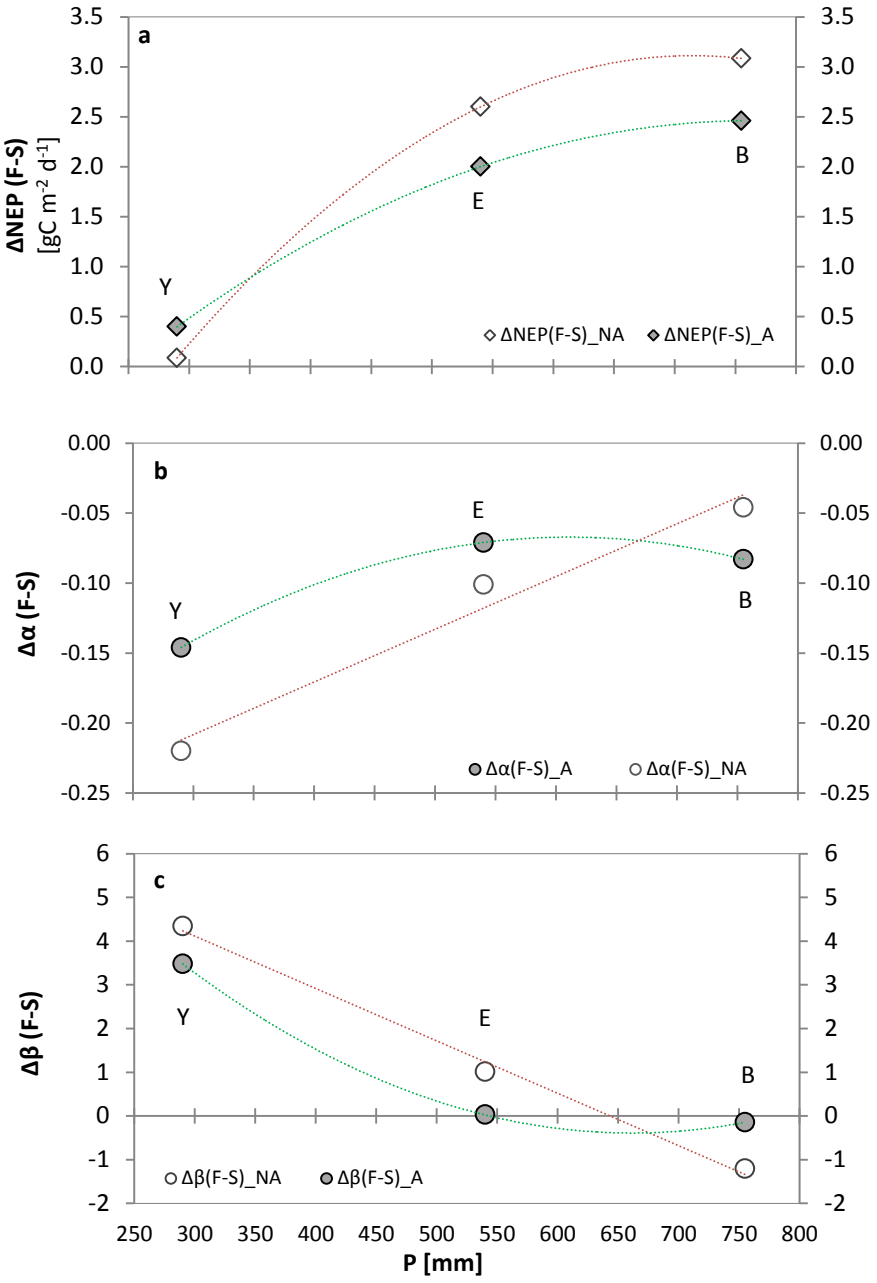

Fig. 11. The impact of the forest compared to the background shrub land across the ICG. The average differences in seasonal carbon gain, albedo, and Bowen ratio between the forest and the shrub land (over 2012-2014) as active function of mean inter-annual precipitation across the ICG (Yatir(Y), Eshtaol(E), and Birya(B)) in the active (A) season (solid cycles) and non-active (NA) season (empty cycles): **(active)** seasonal difference in NEP (Positive value indicates active larger carbon sink in the forest compared to shrub land). **(b)** seasonal difference in α. negative value indicates active smaller albedo in the forest compared to shrub land) and **(c)** seasonal differences in β . (Mid-day averages, 10:00-14:00). Positive value indicates greater fraction of energy dissipates as H (over LE) in the forest rather than is the compared shrub land. α-albedo (S↑/S↓); β, Bowen ratio (H/LE), Δ (F-S), difference between forest and background shrub land; ICG, Israeli Climatic Gradient.

Carbon gain differences, ΔNEP(F-S) (Fig.11a) show the expected increase in carbon gain of forests compared with shrub lands along the gradient (ΔNEP, on average: 2.8, 2.3, and 0.2 gC m^{-2} d^{-1}, in Birya, Eshtaol, and Yatir sites) indicating that the increased contribution of forests to the net carbon gain is correlated positively with precipitation and negatively with temperature, consistent with earlier studies (Anderson- Teixeira et al., 2011). In both seasons, ΔNEP values in the humid forests (Birya and Eshtaol) are larger than in the dry Yatir site. Namely, the forests in both Birya and Eshtaol have not only larger carbon sinks compared to the forest in Yatir, but the carbon uptake enhancement of these forests relative to the background shrub land is more significant than in the Yatir site (Fig. 6). A main reason that may address this trend is the increasing temperature and decreasing water availability,

which enhance respiration in the dry site (see Reichstein et al. (2005)). In the dry season (non-active), Yatir forest became a carbon source, of the same magnitude as the shrub land at the same season (Fig.6b and 6d). Note that the relative contribution of the humid forests (Birya, and Eshtaol) to the ΔNEP in the non-active season is greater than that in the active season, although the absolute fluxes are smaller (ΔNEP in non-active season: 1.1, 1.2, and -0.2, in Birya, Eshtaol, and Yatir, respectively). It is expected that enhanced respiration in Birya and Eshtaol shrub lands (positively correlated with precipitation; Fig.6a-c) contributes to increasing the difference in the carbon gain between the land covers at these sites. A reasonable speculation is that this may be enhanced by the higher percentage of the total vegetation that dries out in the shrub land (annual vegetation) than in the forest during the dry season, and larger decrease in assimilation in the shrub land. This indicates the higher sensitivity of production and respiration in shrub lands (the processes which compose carbon gain) to seasonality (Piao et al., 2009). Finally, it is important to notice that number of factors other than temperature and moisture (e.g. soil type, elevation, site history) are known to strongly influence the carbon gain (Magnani et al., 2007), indicating that the observed ΔNEP gradient, is not an inherently obvious result.

As expected, differences in evapotranspiration (LE) were positively correlated with ΔNEP across the gradient. However, this correlation does not include Yatir in the non-active season, when both ecosystems (Forest vs. Shrub land) are carbon sources, sharing almost the same low NEP values, yet the average LE in the forest is significantly higher than in the shrub land. The impact of the Yatir forest is substantial, in terms of evapotranspiration. The relatively high evapotranspiration in the forest compared to the shrub land may be associated with the deeper root system and water mining capacity of the forest (Yaseef et al. (2010)).

The results provide also insights regarding the differences in surface energy budget characteristics between forests and shrub lands along the ICG. Albedo, which refers to shortwave radiation, was relatively invariable between the forests, independent of seasons (~0.12; Charney et al. (1977); Rotenberg and Yakir (2010); see Fig.8a and 8b), but varied considerably among shrub lands and between shrub land and forest at each site (Fig. 8c and 8d). The albedo in the shrub lands across the ICG is negatively correlated with precipitation across the gradient. It seems that the constant forest albedo and the gradient in the shrub land albedo ($\Delta\alpha_{(F-S)}$, Fig.11b) reflected to a significant extent the effects of the shrub lands' soil surfaces. The speculation is that soil type and its optical characteristics changes from bright sandy soil in the south to darker loamy soil in the north. This resulted in $\Delta\alpha_{F-S}$, on average, of: -0.06, -0.09, and -0.18, in Birya, Eshtaol, and Yatir, respectively. $\Delta\alpha_{F-S}$ is consistently negative due to principally lower albedo of the forests than the background shrub lands across the ICG (Campbell and Norman, 1998; Rotenberg and Yakir, 2010). The steep gradient in $\Delta\alpha_{F-S}$ between humid

sites (Birya and Eshtaol) and the dry site (Yatir) reflects mainly the brighter shrub land surface in the desert area. The results also indicate that the sensitivity of $\Delta\alpha$ to seasonal changes is influenced mainly by shrub lands vegetation cover (mostly annuals), which varies between the active season (soil is masked by living shrubs and herbs) and the non-active season (larger fraction of soil is exposed due to dry shrubs). $\Delta\alpha$ values in the non-active are expected to be larger than these in the active season (-0.10, and -0.22 in the non-active season, compared with -0.07 and -0.15 in the active season, in Eshtaol and Yatir, respectively). However, in Birya, where the difference in albedo between ecosystems is relatively small, the effect of seasonal changes on the $\Delta\alpha$ shows an opposite trend, with larger values in active season than in the non-active season ($\Delta\alpha\sim$ -0.08, and -0.05, in the active, and non-active seasons, respectively). This is apparently because on the relatively darker, basaltic, soil in Birya shrub land vegetation cover, being larger in the active season, slightly increases the albedo. Finally, site specific responses of the different soil covers in the shrub lands (dark basaltic soil, moderate rocky soil, and bright desert sand, in Birya, Eshtaol, and Yatir, respectively) allow shrub lands to dominate the $\Delta\alpha$, caused by the increasing differences in albedo from Birya to Yatir, especially in the non-active season.

The albedo effects described above increase the surface solar radiation load in the pine forests compared with the background shrub lands along the ICG (by 22, 19, 39 W m^{-2} in the active season and by 13, 30, 64 W m^{-2} in the non-active season in Birya, Eshtaol, and Yatir, respectively; Table.4). However, it is important to note that the differences in radiation load along the ICG were influenced by the incoming global energy. For example Eg in Yatir was slightly higher compared with Eshtaol and Yatir, regardless of season, which is probably due to lower cloud coverage conditions typical to the environment, and less likely due to latitudinal and altitudinal issues. Considering the differences in non-radiative fluxes, different patterns in H and LE were reflected in the Bowen ratio values (H/LE) along the ICG. The explanation for the Bowen ratio differences between forest and shrub land ($\Delta\beta_{F\text{-}S}$; Fig.11c) is complex and therefore we look first at each component (H and LE) separately. Both sensible heat and latent heat were always higher in the forests compared with shrub land; $\Delta H_{F\text{-}S}\sim$ 45, 40, and 47W m^{-2}, and $\Delta LE_{F\text{-}S}\sim$ 34, 17, and 8W m^{-2}, on average for Birya, Eshtaol, and Yatir sites in active and non-active seasons, respectively (Fig. 9).

Generally, energy fluxes are expected to be greater in the forests due to the higher radiation absorption in the forests compared with shrub land (Betts et al., 2007; Betts, 2000; Bonan, 2008; Rotenberg and Yakir, 2010). Considering the gradient in precipitation along the ICG, $\Delta LE_{F\text{-}S}$ values are expected to increase from dry to wet sites (Anderson- Teixeira et al., 2011). Although the shrub land LE values do not clearly fit the gradient in the active season (Fig.9), the forest LE fluxes overwhelm

these of the shrub land what results in the observed gradient in ΔLE_{F-S}, with largest differences between forest and shrub land in Birya, and the smallest in Yatir. In contrast, the respective average ΔH_{F-S} values do not show a significant trend between the sites. This may be reflected in the Bowen ratio (midday values), when the difference in average β values between the sites (Fig.10) mainly reflected increased differences in LE fluxes.

In order to highlight the differences in Bowen ratio along the gradient, and between the sites, midday values were calculated (Cuenca et al., 2013; Ohmura, 1982). Comparison between the midday (10:00-14:00) and the daily (24h) β averages (β_{Mid}-β_{Day}), in each of the forests and the shrub lands, reveals higher β values in midday (Verma et al., 1986) in all sites and seasons (β_{Mid}-β_{Day} ranged between 0-1.9), except Yatir site. In particular, in Yatir shrub land the negative value was observed during the non-active season (β_{Mid}-β_{Day}~ -4.5). In this case, daily mean H was about 30% of the midday H, whereas the daily mean LE was ~10% of the comparable midday. This is reflected by time shift of LE fluxes later to the afternoon together with negative LE fluxes during night time (Yaseef et al., 2010). In Yatir forest, the differences were much larger than in other forests (β_{Mid}-β_{Day}~ 2.8 and 9.3, in the active and the non-active season, respectively). This indicates that Yatir forest, in contrast to other forests and shrub lands along ICG, extremely enhanced H fluxes during midday, with even larger effect during the dry season, reflecting the unique "convector effect", which occurs during the high radiation time of the midday (Rotenberg and Yakir, 2010, 2011). $\Delta\beta_{F-S}$ values in Fig.11c are in agreement with the observed albedo effect and are negatively correlated with the precipitation gradient. In general, the main difference in Δβ across the ICG is between the dry Yatir and the humid sites of Birya and Eshtaol. Note that the midday β values in Yatir site are considerably higher compared to Birya and Eshtaol sites, in both, forests and shrub lands (Fig.10). This emphasizes the transition from relatively high LE fluxes in the humid sites to the extremely small LE fluxes in the dry desert of Yatir (Cavanaugh et al., 2011). Note that to understand better the impact of land cover on the Bowen ratio along the ICG we examined the differences in midday values, $\Delta\beta_{F-S}$ (Fig.11c), in both seasons (active and non-active). This is in contrast with other variables, where daily values were applied. $\Delta\beta_{F-S}$ decreases with increasing precipitation along the ICG, in both seasons. The positive $\Delta\beta_{F-S}$ values in Yatir and Eshtaol indicated that compared with the shrub land, the forest releases a larger fraction of the available energy through a sensible heat flux (H) rather than through latent heat (LE) flux, corresponding with decreased water availability, in Eshtaol site and more significantly in Yatir site, and with decreased albedo in the forests compared with the shrub land. Thus, the changes in Bowen ratio are consistent also with the small negative $\Delta\beta_{F-S}$ in Birya, in both seasons. In this case water availability is higher, compared with Yatir and Eshtaol sites, and consequently the preference of H flux

over LE flux in both forest and shrub land, is similar. This correlated with the main trend in forest vs. shrub land differences across the ICG; $\Delta\beta$ decreases with decreasing $\Delta\alpha$ due to reduced solar radiation load effect in the forests and reduced demand for H flux compared to the shrub land. $\Delta\beta$ also decreases with increasing precipitation due to increased water availability from Yatir to Birya. As mentioned above, extremely high $\Delta\beta$ in Yatir, compared to Birya and Eshtaol, is associated with the strong suppression of LE in the forest during midday in the dry site. This is compensated by the highly efficient H flux, termed the "convector effect", enhanced by efficient canopy-atmosphere aerodynamic coupling due the open, low density canopy in Yatir (Rotenberg and Yakir (2010)). In the Yatir shrub land, this effect is less significant than in the forest due to lower available energy (higher α), and lower surface-atmosphere aerodynamic coupling (larger r_a; see introduction), which in turn suppressed H flux. This mechanism explains the decrease of $\Delta\beta$ values in Eshtaol and more in Birya (e.g. in Birya, the smaller $\Delta\alpha$ is correlated with higher precipitation, and the decreasing r_a correlated with increasing density of forest's canopy). The negative $\Delta\beta$ in Birya in the non-active season reflects that the forest dissipate larger LE flux (relatively to H flux), compared with the background shrub land (due to dry shrubs and no water availability). However the sensitivity of $\Delta\beta$ to seasonality in Birya (diminishing differences in β between forest to shrub land in the active season) can be explained by enhanced vegetation growth in the shrub land during more wet active season (LE increases together with decreases of H in shrub land in the active season, compared with the non-active season; Fig.9c-d, Fig.9g-h) which leads to an increase in Birya shrub land α in the active season (increased $\Delta\alpha$ in Birya in the active season), but to high decrease of shrub land β (decreased $\Delta\beta$ in Birya in the active season).

The above differences in carbon and energy net exchanges between forests to shrub lands have an important role in shaping the net radiation load associated with forestation in different environmental and climatic regions. For understanding the offset between these effects, we quantified also the shortwave and the longwave radiations load associated with forestation across the ICG in Table 4.

Table 4.The estimated radiation effect of forestation along the ICG. Global radiation (S↓) is the average value for the forest during the study period, in each of the seasons. Albedo differences presented as absolute values, when forest always have lower albedo than shrub land. Net radiation values refer to the ecosystem surface. Net shortwave (solar) radiation (ΔS_n) shows the difference in surface's solar load between the forest and the shrub land (positive sign denotes higher solar radiation load in the forest canopy, on average). ΔS_n values were derived by the measured albedo in each forest and shrub land, together with the measured global radiation above the forests at the same period. Net longwave (thermal) radiation (ΔL_n) presents the corresponding differences in surface's thermal load (negative sign denotes less emission of longwave radiation from the forest canopy, compared with the shrub land). **the estimated effect for the selected measurement window (using the measured S↓ and the Δα).*

Season	**Active**			**Non-Active**		
Site	B	E	Y	B	E	Y
Global radiation *(S↓),[W m^{-2}]*	270	225	280	301	308	306
Δ(F-S)						
Albedo difference *(|Δα|)*	0.08	0.07	0.15	0.05	0.10	0.22
Difference in net shortwave *$\Delta S_n=S_{n(F)}- S_{n(S)}$, [Wm^{-2}]**	22	16	41	14	31	67
Difference in net longwave *$\Delta L_n=\|L_{n(F)}\|-\|L_{n(S)}\|$,[Wm^{-2}]*	-3	1	-22	6	-20	-18
Difference in net radiation ΔRn	**25**	**15**	**63**	**8**	**51**	**85**

As can be seen in Table.4, the differences in the net shortwave radiation between the ecosystems (F vs. S) across the ICG sites indicate that the forests were always greater absorbers of solar radiation compared to their background shrub land. The increasing differences in net shortwave radiation from Birya to Yatir are mainly due to the increased differences in albedo between forest and shrub land. The insignificant increase in global radiation from Birya to Yatir has only a small contribution to the observed higher radiation in Yatir. Note that the relatively small ΔS_n value in Eshtaol in the active season clearly results from the relatively small global radiation average value (225W m^{-2}), probably caused due to cloudiness during the period of measurement. The effect of forests on thermal radiation (ΔL_n) also increases from Birya to Yatir (on average, from ~3 to -20W m^{-2}, in Birya and Yatir, respectively) implying that the convector effect (Rotenberg and Yakir, 2010, 2011) observed in the dry forest of Yatir is diminishing across the gradient sites, from Yatir to Birya. While reduced emission of thermal radiation associated with forestation is clear in Yatir, it is almost zero in Birya. The difference in net radiation highlights the higher impact of forestation on the surface's radiation load in Yatir, compared with forestation in the other sites across the ICG sites.

The forestation along the ICG provides an insight on how different climate (precipitation and temperature) and land cover changes interact with the atmosphere-biosphere processes. The use of the mobile system demonstrated its critical utility for the extension of the results from the permanent research site, in Yatir with limited coverage of climatic conditions, land cover and vegetation types.

As shown here, the vegetation land cover affects the interactions between the ecosystem and the atmosphere not only through the exchange of carbon but also through the different radiation absorption/reflection/emission by the surface, as well as its redistribution to the atmosphere as non-radiative fluxes of latent heat and sensible heat. The tradeoff between the net effects of these processes provides insights regarding the contribution of forestation and land use changes, in general, to climate change on local to global scales.

Our observations from the semi-arid region in Israel showed that conversion of the local sparse shrub land to pine forest resulted in greatly increased surface radiation load due to reduced canopy albedo and reduced emission of thermal radiations, which overwhelmed the beneficial effects of the forests high rates of carbon sequestration (which can be converted into energy term, see (Rotenberg and Yakir (2010)). The tradeoff between these processes results in a net warming effect associated with forestation in Yatir. Extending this study to three pine forests across the short (180 km) local climatic gradient in Israel, confirmed our hypothesis that increased carbon sequestration and reduced differences in albedo across the precipitation gradient (from Yatir to Birya), diminish the radiation load effect of forestation while enhancing the benefits of carbon sequestration. This suggests that the warming effect associated with forestation decreases with increasing precipitation across the ICG sites to the extent that at Birya the warming effect is not sustained.

5 References

Anderson- Teixeira, K. J., Delong, J. P., Fox, A. M., Brese, D. A., and Litvak, M. E. (2011). Differential responses of production and respiration to temperature and moisture drive the carbon balance across a climatic gradient in New Mexico. *Global Change Biology* **17**, 410-424.

Asaf, D., Rotenberg, E., Tatarinov, F., Dicken, U., Montzka, S. A., and Yakir, D. (2013). Ecosystem photosynthesis inferred from measurements of carbonyl sulphide flux. *Nature Geoscience* **6**, 186-190.

Austin, A. T. (2002). Differential effects of precipitation on production and decomposition along a rainfall gradient in Hawaii. *Ecology* **83**, 328-338.

Ballantyne, A., Alden, C., Miller, J., Tans, P., and White, J. (2012). Increase in observed net carbon dioxide uptake by land and oceans during the past 50 years. *Nature* **488**, 70-72.

Beer, C., Reichstein, M., Tomelleri, E., Ciais, P., Jung, M., Carvalhais, N., Rödenbeck, C., Arain, M. A., Baldocchi, D., and Bonan, G. B. (2010). Terrestrial gross carbon dioxide uptake: global distribution and covariation with climate. *Science* **329**, 834-838.

Betts, A. K., Desjardins, R. L., and Worth, D. (2007). Impact of agriculture, forest and cloud feedback on the surface energy budget in BOREAS. *Agricultural and forest meteorology* **142**, 156-169.

Betts, R. A. (2000). Offset of the potential carbon sink from forestation by decreases in surface albedo. *Nature* **408**, 187-190.

Bonan, G. B. (2008). Forests and climate change: forcings, feedbacks, and the climate benefits of forests. *science* **320**, 1444-1449.

Brovkin, V., Sitch, S., Von Bloh, W., Claussen, M., Bauer, E., and Cramer, W. (2004). Role of land cover changes for atmospheric CO2 increase and climate change during the last 150 years. *Global Change Biology* **10**, 1253-1266.

Campbell, G. S., and Norman, J. M. (1998). An introduction to environmental biophysics.

Canadell, J. G., Le Quéré, C., Raupach, M. R., Field, C. B., Buitenhuis, E. T., Ciais, P., Conway, T. J., Gillett, N. P., Houghton, R., and Marland, G. (2007). Contributions to accelerating atmospheric CO2 growth from economic activity, carbon intensity, and efficiency of natural sinks. *Proceedings of the National Academy of Sciences of the United States of America* **104**, 18866-18870.

Cavanaugh, M. L., Kurc, S. A., and Scott, R. L. (2011). Evapotranspiration partitioning in semiarid shrubland ecosystems: a two-site evaluation of soil moisture control on transpiration. *Ecohydrology* **4**, 671-681.

Charney, J., Quirk, W. J., Chow, S.-H., and Kornfield, J. (1977). A comparative study of the effects of albedo change on drought in semi-arid regions. *Journal of the Atmospheric Sciences* **34**, 1366-1385.

Claussen, M., Brovkin, V., and Ganopolski, A. (2001). Biogeophysical versus biogeochemical feedbacks of large-scale land cover change. *Geophysical research letters* **28**, 1011-1014.

Conant, R. T., Klopatek, J. M., Malin, R. C., and Klopatek, C. C. (1998). Carbon pools and fluxes along an environmental gradient in northern Arizona. *Biogeochemistry* **43**, 43-61.

Cubasch, U., Wuebbles, D., Chen, D., Facchini, M. C., Frame, D., Mahowald, N., and Winther, J.-G. (2013). Introduction. *In* "Climate Change 2013: The Physical Science Basis. Contribution of Working Group I to the Fifth Assessment Report of the Intergovernmental Panel on Climate Change" (T. F. Stocker, D. Qin, G.-K. Plattner, M. Tignor, S. K. Allen, J. Boschung, A. Nauels, Y. Xia, V. Bex and P. M. Midgley, eds.), pp. 119–158. Cambridge University Press, Cambridge, United Kingdom and New York, NY, USA.

Cuenca, R. H., Ciotti, S. P., and Hagimoto, Y. (2013). Application of Landsat to evaluate effects of irrigation forbearance. *Remote Sensing* **5**, 3776-3802.

Davin, E., de Noblet-Ducoudré, N., and Friedlingstein, P. (2007). Impact of land cover change on surface climate: Relevance of the radiative forcing concept. *Geophysical Research Letters* **34**.

Feng, Y., Ramanathan, V., and Kotamarthi, V. (2013). Brown carbon: a significant atmospheric absorber of solar radiation? *Atmospheric Chemistry and Physics* **13**, 8607-8621.

Field, C. B., and Raupach, M. R. (2004). "The global carbon cycle: integrating humans, climate, and the natural world," Island Press.

Foken, T., Aubinet, M., and Leuning, R. (2012). Eddy Covariance: A particular Guide to Measurment and Data Analysis, pp. 1-19. Springer.

Foster, G., and Rahmstorf, S. (2011). Global temperature evolution 1979–2010. *Environmental Research Letters* **6**, 044022.

Grünzweig, J., Lin, T., Rotenberg, E., Schwartz, A., and Yakir, D. (2003). Carbon sequestration in arid-land forest. *Global Change Biology* **9**, 791-799.

Holzapfel, C., Tielbörger, K., Parag, H. A., Kigel, J., and Sternberg, M. (2006). Annual plant–shrub interactions along an aridity gradient. *Basic and Applied Ecology* **7**, 268-279.

Jones, H. G. (1992). "Plants and microclimate," second edition/Ed. CAMBRIDGE.

Kiehl, J., and Trenberth, K. E. (1997). Earth's annual global mean energy budget. *Bulletin of the American Meteorological Society* **78**, 197-208.

Le Quéré, C., Raupach, M. R., Canadell, J. G., and Marland, G. (2009). Trends in the sources and sinks of carbon dioxide. *Nature Geoscience* **2**, 831-836.

Liu, H., and Foken, T. (2001). A modified Bowen ratio method to determine sensible and latent heat fluxes. *Meteorologische Zeitschrift* **10**, 71-80.

Ma, Y., Su, Z., Li, Z., Koike, T., and Menenti, M. (2002). Determination of regional net radiation and soil heat flux over a heterogeneous landscape of the Tibetan Plateau. *Hydrological Processes* **16**, 2963-2971.

Magnani, F., Mencuccini, M., Borghetti, M., Berbigier, P., Berninger, F., Delzon, S., Grelle, A., Hari, P., Jarvis, P. G., and Kolari, P. (2007). The human footprint in the carbon cycle of temperate and boreal forests. *Nature* **447**, 849-851.

Monteith, J. (1965). Evaporation and environment. *In* "Symp. Soc. Exp. Biol", Vol. 19, pp. 4.

Monteith, J., and Unsworth, M. (1990). "Principles of environmental physics."

Montgomery, R. (1948). Vertical eddy flux of heat in the atmosphere. *Journal of Meteorology* **5**, 265-274.

Myhre, G., Shindell, D., Bréon, F.-M., Collins, W., Fuglestvedt, J., Huang, J., Koch, D., Lamarque, J.-F., Lee, D., Mendoza, B., Nakajima, T., Robock, A., Stephens, G., Takemura, T., and Zhang, H. (2013). Anthropogenic and Natural Radiative Forcing. *In* "Climate Change 2013: The Physical Science Basis. Contribution of Working Group I to the Fifth Assessment Report of the Intergovernmental Panel on Climate Change" (T. F. Stocker, D. Qin, G.-K. Plattner, M. Tignor, S. K. Allen, J. Boschung, A. Nauels, Y. Xia, V. Bex and P. M. Midgley, eds.), pp. 659–740. Cambridge University Press, Cambridge, United Kingdom and New York, NY, USA.

Ne'eman, G., and Trabaud, L. (2000). "Ecology, biogeography and management of Pinus halepensis and P. brutia forest ecosystems in the Mediterranean Basin," Backhuys Publishers Postbus 321, 2300 AH Leiden, The Netherlands.

Obukhov, A., and Yaglom, A. (1959). On the microstructure of atmospheric turbulence–A review of recent work in the USSR. *Quarterly Journal of the Royal Meteorological Society* **85**, 81-90.

Ohmura, A. (1982). Objective criteria for rejecting data for Bowen ratio flux calculations. *Journal of Applied Meteorology* **21**, 595-598.

Otterman, J. (1974). Baring high-albedo soils by overgrazing- A hypothesized desertification mechanism. *Science* **186**, 531-533.

Pan, Y., Birdsey, R. A., Fang, J., Houghton, R., Kauppi, P. E., Kurz, W. A., Phillips, O. L., Shvidenko, A., Lewis, S. L., and Canadell, J. G. (2011). A large and persistent carbon sink in the world's forests. *Science* **333**, 988-993.

Piao, S., Friedlingstein, P., Ciais, P., Peylin, P., Zhu, B., and Reichstein, M. (2009). Footprint of temperature changes in the temperate and boreal forest carbon balance. *Geophysical Research Letters* **36**.

Ramanathan, V., Barkstrom, B. R., and Harrison, E. F. (2008). Climate and the Earth's radiation budget. *Physics Today* **42**, 22-32.

Reichstein, M., Falge, E., Baldocchi, D., Papale, D., Aubinet, M., Berbigier, P., Bernhofer, C., Buchmann, N., Gilmanov, T., and Granier, A. (2005). On the separation of net ecosystem exchange into assimilation and ecosystem respiration: review and improved algorithm. *Global Change Biology* **11**, 1424-1439.

Rotenberg, E., and Yakir, D. (2010). Contribution of semi-arid forests to the climate system. *Science* **327**, 451-454.

Rotenberg, E., and Yakir, D. (2011). Distinct patterns of changes in surface energy budget associated with forestation in the semiarid region. *Global change biology* **17**, 1536-1548.

Schimel, D. S. (1995). Terrestrial ecosystems and the carbon cycle. *Global change biology* **1**, 77-91.

Schwiebus, A., and Berger, F. H. (2005). Sensitivity studies and their application to infer surface energy fluxes: prospects within the passive remote sensing. *Physics and Chemistry of the Earth, Parts A/B/C* **30**, 187-193.

Solomon, S. (2007). Climate change 2007-the physical science basis: Working group I contribution to the fourth assessment report of the IPCC.

Steffen, W., Crutzen, P. J., and McNeill, J. R. (2007). The Anthropocene: are humans now overwhelming the great forces of nature. *Ambio: A Journal of the Human Environment* **36**, 614-621.

Stull, R. B. (1988). "An introduction to boundary layer meteorology," Springer.

Swinbank, W. (1951). The measurement of vertical transfer of heat and water vapor by eddies in the lower atmosphere. *Journal of Meteorology* **8**, 135-145.

Twine, T. E., Kustas, W., Norman, J., Cook, D., Houser, P., Meyers, T., Prueger, J., Starks, P., and Wesely, M. (2000). Correcting eddy-covariance flux underestimates over a grassland. *Agricultural and Forest Meteorology* **103**, 279-300.

Verma, S. B., Baldocchi, D. D., Anderson, D. E., Matt, D. R., and Clement, R. J. (1986). Eddy fluxes of CO2, water vapor, and sensible heat over a deciduous forest. *Boundary-Layer Meteorology* **36**, 71-91.

Whittaker, R. H., and Niering, W. A. (1975). Vegetation of the Santa Catalina Mountains, Arizona. V. Biomass, production, and diversity along the elevation gradient. *Ecology*, 771-790.

Wilson, K., Goldstein, A., Falge, E., Aubinet, M., Baldocchi, D., Berbigier, P., Bernhofer, C., Ceulemans, R., Dolman, H., and Field, C. (2002). Energy balance closure at FLUXNET sites. *Agricultural and Forest Meteorology* **113**, 223-243.

Yaseef, N. R., Yakir, D., Rotenberg, E., Schiller, G., and Cohen, S. (2010). Ecohydrology of a semi-arid forest: partitioning among water balance components and its implications for predicted precipitation changes. *Ecohydrology* **3**, 143-154.